Technical Training Notes in Ground-Water Hydrology: Radial Flow to a Well

by: Gordon D. Bennett, Thomas E. Reilly, and Mary C. Hill

U.S. Geological Survey
Water Resources Investigations Report 89—4134

April 1990

DEPARTMENT OF THE INTERIOR

MANUEL LUJAN, JR., Secretary

U.S. GEOLOGICAL SURVEY

Dallas L. Peck, Director

For additional information, write to:

U.S. Geological Survey
Office of Ground Water
411 National Center
Reston, Virginia 22092
Telephone: (703) 648-5001

Copies of the report can be purchased from:

U.S. Geological Survey
Books and Open-File Reports
Box 25425, Federal Center
Denver, Colorado 80225

CONTENTS

	Page
Preface	vii
Abstract	1
Introduction	1
General characteristics of radial flow	2
Lateral hydraulic conductance in radial flow	6
Discretization in nonequilibrium flow simulation in the r-z plane	9
Lateral conductance	14
Vertical conductance	14
Storage capacity	17
Radial-Flow Problem	18
Model design	19
Stream functions	23
Flow-net construction	24
Flow-net interpretation	34
Estimation of lateral hydraulic conductivity from pumpage response data	35
Specific-capacity analysis	35
Distance-drawdown analysis	36
Time of travel calculation	37
Note on transient response	40
Summary	41
Appendixes	43
A-I Derivation of flow equations--axially symmetric flow r-z plane	43
A-II Water-table storage as a boundary condition	48
A-III Approximation of the flow equation in the radial flow model	51
A-IV Answers to exercises and the radial-flow problem	59
References	83

List of Figures

		Page
Figure 1.	A cross section showing a well tapping a confined aquifer at the center of an island	3
Figure 2.	Diagram showing the cross-sectional area of flow at a radius r from the well of Figure 1	4
Figure 3.	Diagram showing the decrease in cross-sectional area with decreasing radius	4
Figure 4.	Diagram showing a cylindrical shell for calculation of hydraulic conductance using log formula	7
Figure 5.	Diagram showing a shell for hydraulic conductance calculation using distance and area of flow	7
Figure 6.	Diagram showing the hydraulic conductance of finite cylindrical shell as an integration of elemental shells in series	10
Figure 7.	Cross section showing flow net in the r-z plane for axially symmetric flow to a well sustained by uniform recharge to the water table	12
Figure 8.	Diagram showing node array in the r-z plane	12
Figure 9.	Diagram showing shells used for definition of hydraulic conductance and storage capacity in axially symmetric flow	13
Figure 10.	Diagram showing cylindrical shell extending inward and outward from the node column at radius r_a	16
Figure 11.	Top review of cylindrical shell extending inward and outward from the node column at radius r_a	16
Figure 12.	Schematic of hydrologic conditions for the radial-flow problem	20
Figure 13.	Cross section showing model node array and volume elements used in calculating simulation coefficients	22
Figure 14.	Cross section showing flownet in the r-z plane for axially symmetric flow to a well	25
Figure 15.	Diagram of node array and lateral hydraulic conductance blocks for stream function calculation	26
Figure 16.	Node array showing head values	28
Figure 17.	Cross section of stream tube segment showing mean radius, r, from well axis	39

Page

Figure A-1. Diagram showing cylindrical element volume illustrating axially symmetric flow.....44

Figure A-2. Graph showing plot of the function $r(\partial h/\partial r)$ against r.....46

Figure A-3. Graph showing the finite difference approximation of $\partial^2 h/\partial(\ln r)^2$ at node i,j.....52

Figure A-4. Diagram showing cylindrical element volume containing the node i,j.....54

Figure A-5. Answers shown on model node array and volume elements used in calculating simulation coefficients.....67

Figure A-6. Answers for stream-function calculations shown on model array and lateral conductance blocks.....70

Figure A-7. Cross section of radial-flow net.....72

Figure A-8. Distance - drawdown graph.....77

Figure A-9. Graph of 0.4 to 0.5 flow tube used to calculate areas for time of travel.....82

List of Tables

Table 1 - Worksheet for calculation of radial hydraulic conductance.....10

Table 2 - Worksheet for the calculation of stream functions.....32

Table A-1 - Table 2 answers.....68

PREFACE

An important activity of the U.S. Geological Survey is the dissemination of technical information related to water resources. A small but significant part of this technical information consists of informal unpublished documents that supplement available published reports and specifically relate to or are relevant for technical training of water-resources professionals. Although many of these training documents are very narrowly focused, it is useful to publish some of them as the need or opportunity arises in order for the information to become more widely available. This report is one of these training doucments. These documents, which focus on narrowly defined elements of ground-water hydrology, will be useful for training water-resources professionals, either in formal training courses, technical workshops or self study.

TECHNICAL TRAINING NOTES IN GROUND-WATER HYDROLOGY: RADIAL FLOW TO A WELL

by

GORDON D. BENNETT, THOMAS E. REILLY, AND MARY C. HILL

ABSTRACT

The theory of radial, or axially-symmetric, ground-water flow to a well is an important specialized topic of ground-water hydraulics. This training note develops the basic concepts of radial flow and its representation in numerical models. A number of problems to be solved by the reader are included with answers to the problems provided at the end of the text. The discussion focuses on the physical characteristics of the radial flow system in the vicinity of a well, particularly those characteristics that are common to most well-aquifer systems; the concepts of finite difference simulation and flow-net analysis are used to illustrate these characteristics. This training note does not include detailed discussion of the various solutions to the differential equations for nonequilibrium flow to a well, as this would exceed its intended scope.

INTRODUCTION

A knowledge of the hydraulics of flow to wells is essential to the study of ground-water flow systems. The reasons for this are twofold: first, wells provide the mechanism through which a large part of the discharge from the ground-water system occurs; second, observation and testing of the ground-water regime, whether related to hydraulics or water quality, usually takes place through wells of some sort.

The purpose of this training note is to explain the physical principles governing ground-water flow to a well. The material reviews and builds upon the basic concepts of radial flow as given, for example, in Bennett (1976, p. 34-52). Emphasis has been placed on those characteristics of the radial flow pattern that are common to most well-aquifer systems; the concepts of finite-difference simulation and flow net analysis are utilized to illustrate these characteristics. Discussions of the various solutions to the differential equations of transient radial flow are not included, as this would exceed the intended scope of this document.

The term "radial flow," as used in this report, denotes axially symmetric flow toward a well--that is, flow which is directed toward a well coaxial with the z (vertical) axis of the cylindrical coordinate system, and is symmetrical about that axis, so that the angular coordinate need not appear in the flow equations.

GENERAL CHARACTERISTICS OF RADIAL FLOW

Figure 1 shows a well located at the center of a circular island. This well taps a confined aquifer which crops out along the island's perimeter, where it is exposed to the head of the surrounding water, h_e. The radius of the island is designated r_e. The well is pumped at a rate Q_w, and horizontal flow occurs radially inward from the perimeter of the island to the well. No vertical flow occurs. Because the island is circular and the well is at its center, the problem exhibits radial symmetry--that is, at a given radial distance from the well, the same condition will prevail in any direction; moreover, the assumption of horizontal flow makes it unnecessary to consider variations in the vertical. Thus, if polar or cylindrical coordinates (figure 1) are used, only one coordinate, the radial distance (r) from the axis of the well, need appear in our equations (see Bennett, 1976, Part III for a more complete discussion).

Flow is in the negative r direction--that is, inward along the r axis. The cross-sectional area of flow at any radius, r, is an area perpendicular to the flow direction; thus it is a cylindrical surface extending through the aquifer at the radius r, as shown in figure 2. If the thickness of the aquifer is b, the magnitude of this area at any radius is simply $2\pi br$. So this problem is one in which the cross sectional area of flow changes along the flow path, becoming progressively smaller as we approach the well, as shown in figure 3.

We now apply Darcy's law to the flow crossing the cylindrical area of figure 2. We are dealing with a steady-state situation, with no storage effects; the discharge entering the aquifer along the perimeter of the island is the same as that entering the well, and the flow across any cylindrical surface coaxial with the well has this same value, Q_w. Thus, Darcy's law for flow across the surface shown in figure 2 is simply

$$Q_w = -K(\text{area})\frac{dh}{dr} = -K \cdot 2\pi br \frac{dh}{dr} \qquad (1)$$

where $\frac{dh}{dr}$ is the gradient of head in the r direction--i.e., in the direction opposite to the flow. If we maintain strict sign conventions, the discharge of the well, Q_w, must be treated as a negative quantity, since it is directed inward, in the direction of decreasing r. However, we will think of well discharge as a positive term. With the understanding that Q_w will be considered positive, therefore, we drop the negative sign on the right side of (1) obtaining

$$Q_w = 2\pi Kbr \frac{dh}{dr} \qquad (2)$$

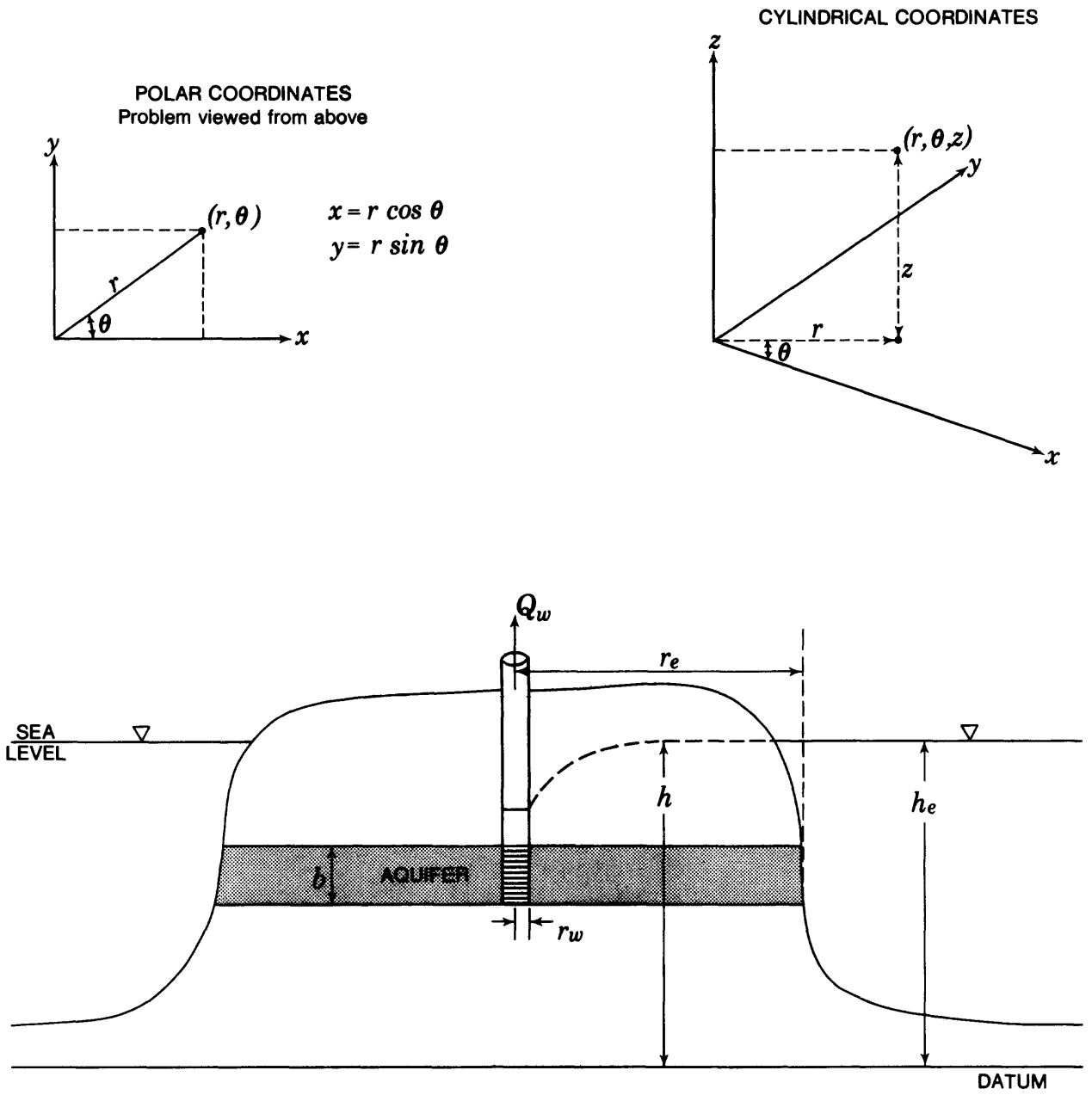

Figure 1 - A well tapping a confined aquifer at the center of an island. Horizontal flow occurs radially inward from the perimeter of the island to the well. Thus, flow is in the negative r direction.

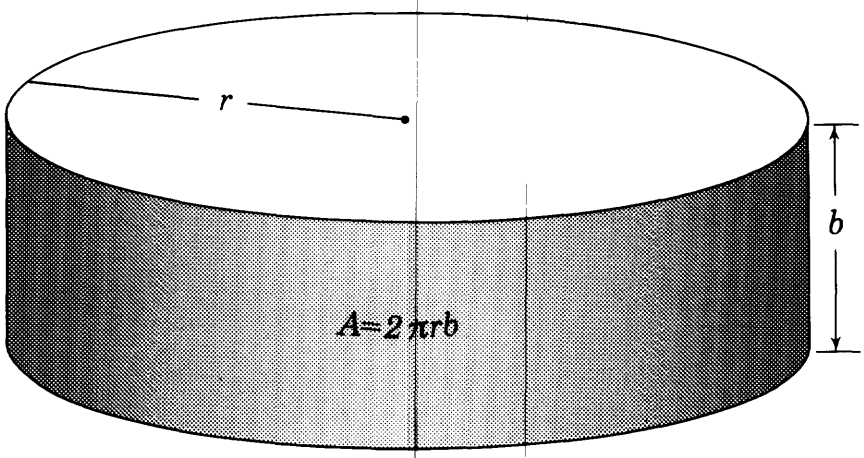

Figure 2 - Cross-sectional area of flow at a radius r from the well of fig. 1.

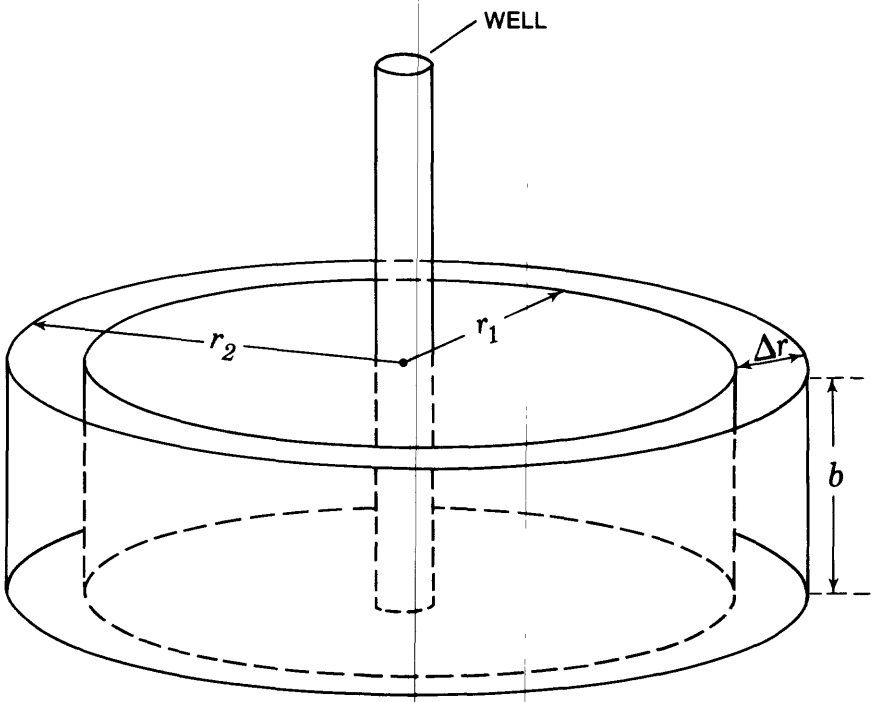

Figure 3 - Decrease in cross-sectional area with decreasing radius.

The discharge Q_w is the same for any value of r we choose; thus the left side of the equation is a constant. On the right side of the equation, the terms 2, π, b and K are all constant; thus for the right side as a whole to remain constant, $\frac{dh}{dr}$ must increase as r decreases. In other words, to compensate for the progressive decrease in flow area, the gradient must steepen progressively as we approach the well. This is the cause of the familiar drawdown "cone," or "cone of depression," in the water levels surrounding a pumping well; close to the well, flow areas become very small, and hydraulic gradients must become correspondingly steep.

Equation (2) is a differential equation which we can rearrange as

$$\frac{dh}{dr} = \frac{Q_w}{2\pi Kb} \frac{1}{r} . \qquad (3)$$

Exercise 1: differentiate the equation

$$h = \frac{Q_w}{2\pi Kb} \ln r + C \qquad (4)$$

to show that it is a solution to the differential equation (3). C is a constant.

Thus, (4) can be shown to be a solution of (3). Equation (4) must also address the boundary condition of the problem--that at the radius of the island, r_e, head is equal to h_e. This can be done by properly defining c as follows.

At r_e we know that the following must be true:

$$h_e = \frac{Q_w}{2\pi Kb} \ln r_e + C.$$

Equation (4) will satisfy the boundary condition if:

$$C = h_e - \frac{Q_w}{2\pi Kb} \ln r_e.$$

Thus, we have

$$h = h_e - \frac{Q_w}{2\pi Kb} (\ln r_e) + \frac{Q_w}{2\pi Kb} (\ln r). \qquad (5)$$

Verify that (5) satisfies the boundary condition by substituting h_e and r_e for h and r, respectively.

Equation (5) is one form of the well known Thiem equation. It can of course also be expressed in terms of logarithms to the base 10; using either base, the results show that head in the vicinity of a discharging well varies with the logarithm of radial distance from the well. The problem of flow to a well at the center of an island is a fictitious one, not likely to be encountered in practice. It is used here because it isolates the problem of steady radial flow for consideration, and because the logarithmic variation of head is a characteristic of most problems of flow to a well, at least in the region close to the well.

LATERAL HYDRAULIC CONDUCTANCE IN RADIAL FLOW

In this discussion, our purpose is to use radial flow analysis to focus on the hydraulic conductance, in the radial direction, of a cylindrical shell within the aquifer, such as the one shown in figure 4. The shell extends from an inner radius r_1 to an outer radius r_2. Equation (5) can be applied at the outer surface of the shell by setting r equal to r_2, obtaining

$$h_2 = h_e - \frac{Q_w}{2\pi Kb}(\ln r_e) + \frac{Q_w}{2\pi Kb}(\ln r_2) \qquad (6)$$

Similarly, we can obtain an expression for h_1, the head along the inner surface of the segment, by setting r equal to r_1 in (5).

Exercise 2: Show that if we do this, and subtract the resulting expression for h_1 from equation (6) we obtain

$$h_2 - h_1 = \frac{Q_w}{2\pi Kb}(\ln r_2 - \ln r_1) \qquad (7)$$

The term $(\ln r_2 - \ln r_1)$ can also be written $\ln (r_2/r_1)$, so that (7) can take the form

$$h_2 - h_1 = \frac{Q_w}{2\pi Kb} \ln (r_2/r_1) \qquad (8)$$

In many problems it is helpful to use the concept of hydraulic conductance. The hydraulic conductance of a block of porous material is simply the ratio of the flow rate through the block to the head difference across it. We can calculate a conductance in the radial direction, C_r, across our cylindrical shell by solving (8) for the ratio $Q_w/(h_2-h_1)$, i.e.,

$$C_r = \frac{Q_w}{h_2-h_1} = \frac{2\pi Kb}{\ln(r_2/r_1)} \qquad (9)$$

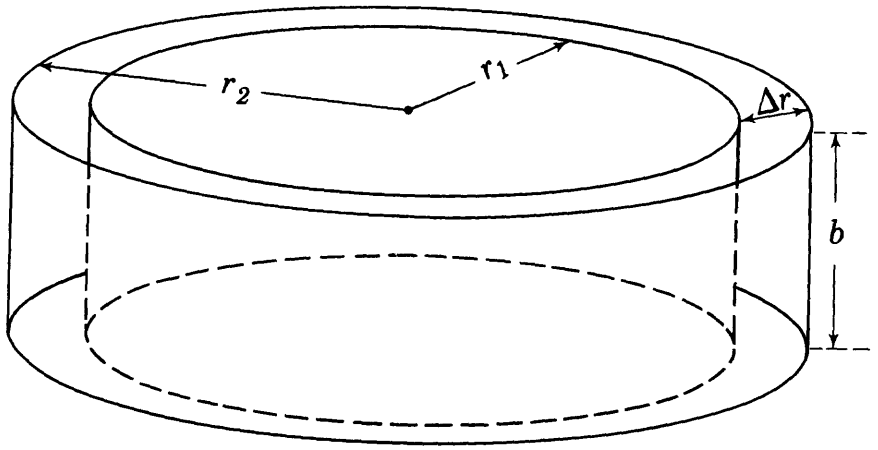

Figure 4 - Cylindrical shell for calculation of hydraulic conductance using log formula

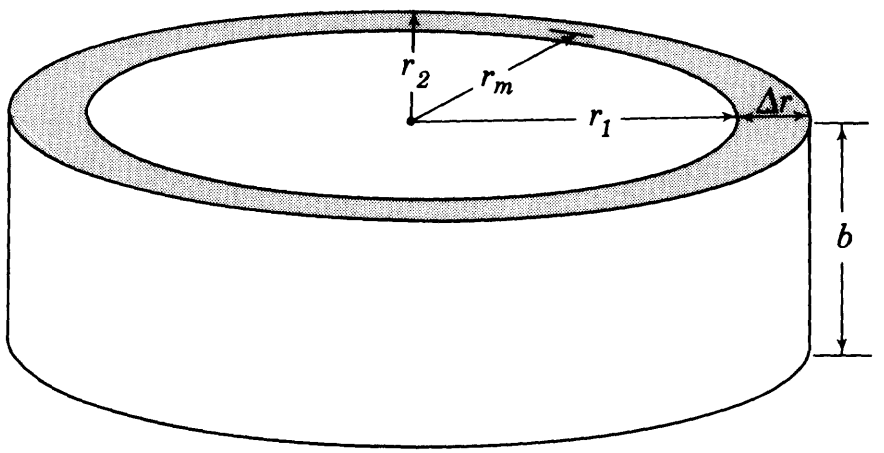

Figure 5 - Shell for hydraulic conductance calculation using distance and area of flow

Equation (9) tells us that two different cylindrical shells will have the same radial hydraulic conductance so long as they have the same ratio of outer to inner radius, r_2/r_1.

In the above approach we have calculated hydraulic conductance as a ratio of flow to computed head loss. Hydraulic conductance may also be approached from a slightly different point of view--that is, using Darcy's law, we may calculate conductance as the product of hydraulic conductivity and cross-sectional flow area, divided by distance of flow (KA/L). Now consider this latter approach in a radial flow problem. Figure 5 shows a cylindrical shell coaxial with the z axis; we wish to calculate hydraulic conductance in the radial direction. The shell has an outer radius r_2, an inner radius r_2, a mean radius r_m (or $\frac{r_1+r_2}{2}$), and a radial width Δr (or $r_2 - r_1$). To calculate hydraulic conductance in the radial direction, we take the distance of flow as Δr. The cross-sectional area actually varies continuously from $2\pi r_2 b$ at the outer radius to $2\pi r_1 b$ at the inner radius; however, we assume that we can use an area calculated at the mean radius, r_m, as a reasonable approximation. This area is simply $2\pi r_m b$, and radial conductance using our formula ($C_r = KA/L$) is therefore

$$C_r = \frac{K \cdot 2\pi r_m b}{\Delta r} \qquad (10)$$

Exercise 3: Table 1 lists values of r_1, r_2, r_m, and Δr for several cylindrical shells, each chosen so that $r_2/r_1 = 2$. Calculate the radial conductance for each shell using equation (10), taking the term $K2\pi b$ as 100 gpd/ft.

Your results should show the same answer, C_r = 150 gpd/ft, for each of the cylindrical segments. The problem illustrates that when the cylindrical shells are chosen in this way, the increase in flow area with increasing distance from the well is offset by a corresponding increase in the distance of flow, Δr, leading to a constant hydraulic conductance. Had we used equation (9) to calculate the radial conductances, we again would have found the same result for each shell, since the ratio r_2/r_1 has the same value for each shell and the log term will thus be the same for each. The calculated results using equation (9) would actually differ by a few percent from those obtained using (10); that is, equation (9) would give a conductance of 144 gpd/ft for each shell, rather than 150 gpd/ft. This is because the use of the mean radius, r_m, to calculate flow area in equation (10) is only an approximation, which becomes exact as Δr tends to zero around r_m. The percentage difference between the two results is related to $\Delta r/r_m$ and the larger the ratio, r_2/r_1, the larger the difference becomes between the two formula.

Finally, we note that equation (9) can be derived from (10) by considering the region between r_1 and r_2 to be occupied by an an infinite number of coaxial cylindrical shells, each of infinitesimal width dr, as shown in figure 6. The conductance of each shell is given by $\frac{2\pi rKb}{dr}$. The shells constitute a set of conductances in series; the conductance of the entire segment from r_1 to r_2 can be obtained assuming one-dimensional flow by applying the rule for conductances in series, which has the form

$$\frac{1}{C_{eq}} = \frac{1}{C_1} + \frac{1}{C_2} + \ldots \frac{1}{C_r} \tag{11}$$

For our case, the form of each term in the summation would be given by

$$\frac{1}{C_i} = \frac{1}{\frac{2\pi r_i Kb}{dr}} \tag{12}$$

The summation thus becomes an integration of the term $\frac{1}{2\pi Kb} \cdot \frac{dr}{r}$ between the limits r_1 and r_2, and the result is identical to equation (9), as the reader may verify. Another very similar approach would be to integrate equation (3) between the limits r_1 and r_2, obtaining (8) as a solution, from which (9) follows.

DISCRETIZATION IN NONEQUILIBRIUM FLOW SIMULATION IN THE R-Z PLANE

We now wish to address the problem of simulating transient flow to a well allowing for vertical as well as radial movement. We use cylindrical coordinates, with the axis of the well taken as the z axis. We assume that symmetry exists around the z axis, so that the angular coordinate, Θ, need not appear in our equations. Thus, we are considering flow which can be fully represented in the r-z plane. Many problems of flow to a partially penetrating well or seepage from a circular pond fall into this category; an example is provided in figure 7, which shows flow lines and lines of equal head in the r-z plane for a well which is screened in an isolated depth interval within an unconfined aquifer, and is supplied by uniform recharge over a circular area of the aquifer's surface.

r_m (ft)	r_1 (ft)	r_2 (ft)	Δr (ft)	C_r (gpd/ft)
1.5	1	2	1	
3	2	4	2	
6	4	8	4	
96	64	128	64	
192	128	256	128	

Table 1 - Worksheet for calculation of radial hydraulic conductance

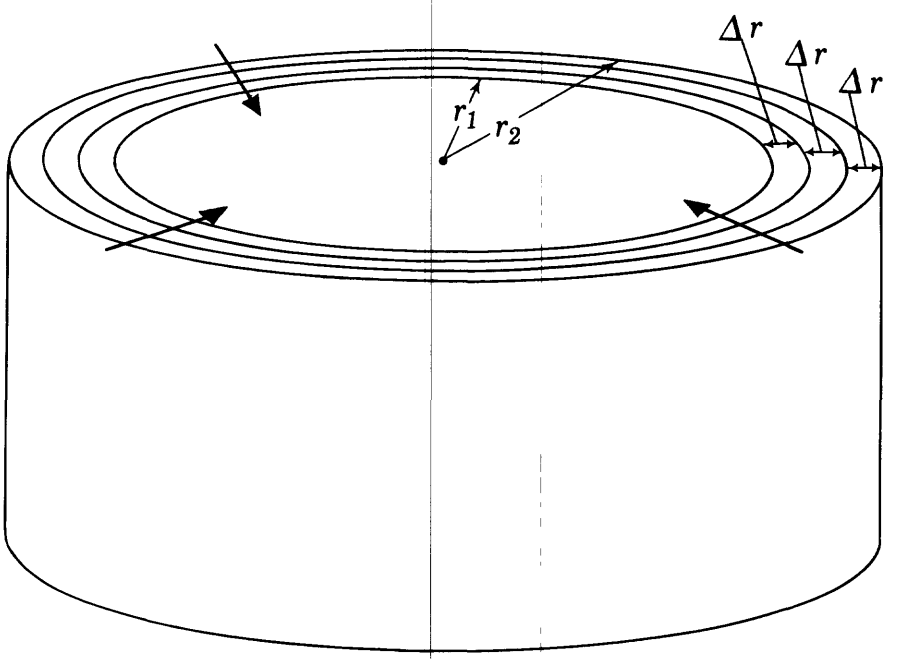

Figure 6 - Hydraulic conductance of finite cylindrical shell as an integration of elemental shells in series

To address problems of this type, we require a method of simulating flow in the r-z plane. Figure 8 illustrates an approach to the problem. A rectangular array of nodes is established in the r-z plane; however, we must keep in mind that we are using the r-z plane to represent three-dimensional flow through a cylindrical section extending from the well radius, r_w, to some outer radius, r_e. Each point on the model plane actually represents a circle extending 360 degrees around the z axis in three-dimensional space; when we consider a rectangular area in the r-z plane, we are actually talking about a cylindrical ring or shell of rectangular cross section, also extending 360 degrees around the z axis; and so on. Along the radial axis of the following problem, we will use an expanding mesh spacing, in which the radius represented by each node will be twice that represented by the node interior to it. The innermost vertical column of nodes falls along the radius of the well, r_w; the outermost column falls on a radius r_e, which ideally should be chosen so as to lie beyond any measurable influence of the well during the period of simulation. Along the vertical axis, spacings are chosen in whatever way the problem requires. (To simplify the present discussion, we will assume that the vertical mesh spacing, Δz, is constant-that is, that the spacing between any two adjacent rows in the mesh is the same. In a subsequent problem, however, we will use two different values of Δz--one in a semiconfining layer, and another in the underlying aquifer.)

Figure 9 shows the system in three dimensions, with a section cut away to show the intersection of the three dimensional flow volume with a vertical plane. In our finite-difference formulation, we will use the face-centered approach--not because it is inherently any better than a block-centered approach, but because it forces us to visualize and formulate conductances as they are actually used in the finite-difference solution process.

Three rectangular areas are shown on figure 9, each representing the instersection of a cylindrical ring or shell of rectangular cross section with the r-z plane. These three cylindrical shells (A, B, and C) represent the volume elements for defining lateral (radial) hydraulic conductance, vertical hydraulic conductance, and storage capacity, respectively. Shell A, which is used for the definition of lateral conductance, extends in the radial direction--i.e., along a row--between two nodes, and extends vertically half the distance to the rows above and below. Shell B, which is used for the definition of vertical conductance extends along the vertical--i.e., along a column--between two nodes, and extends inward and outward to radial distances which are chosen so that the vertical conductance will be equally distributed to either side of the column. This concept is discussed in more detail subsequently. Shell C, is used for the definition of storage capacity, which is defined as the volume of water released from storage in a given volume of aquifer, in response to a unit decline in head within that volume. Note that shell C surrounds a node, extending halfway to the adjacent rows above and below, and extending inward and outward to radial distances chosen so that the storage capacity is equally distributed to either side of the node.

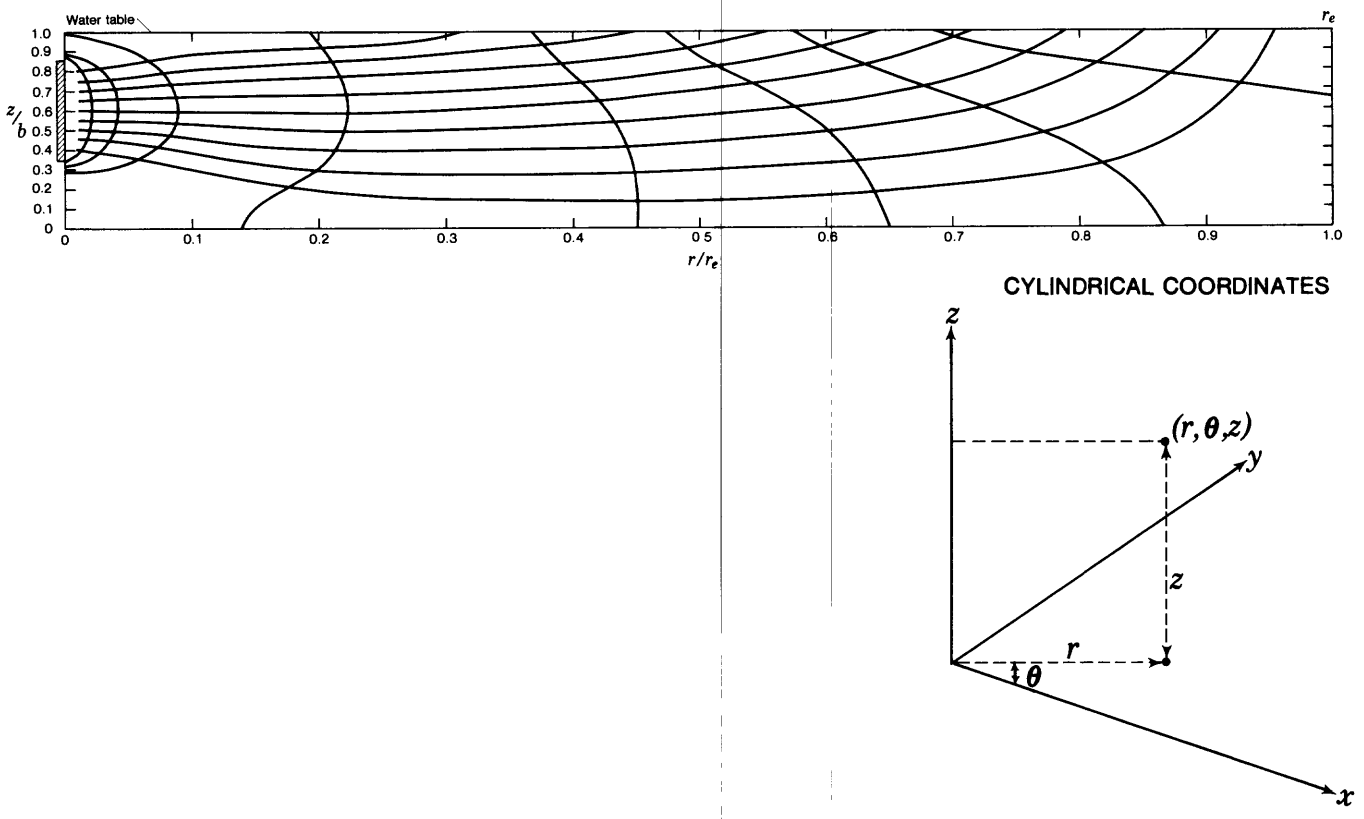

Figure 7 - Flow net in the r-z plane for axially symmetric flow to a well sustained by uniform recharge to the water table

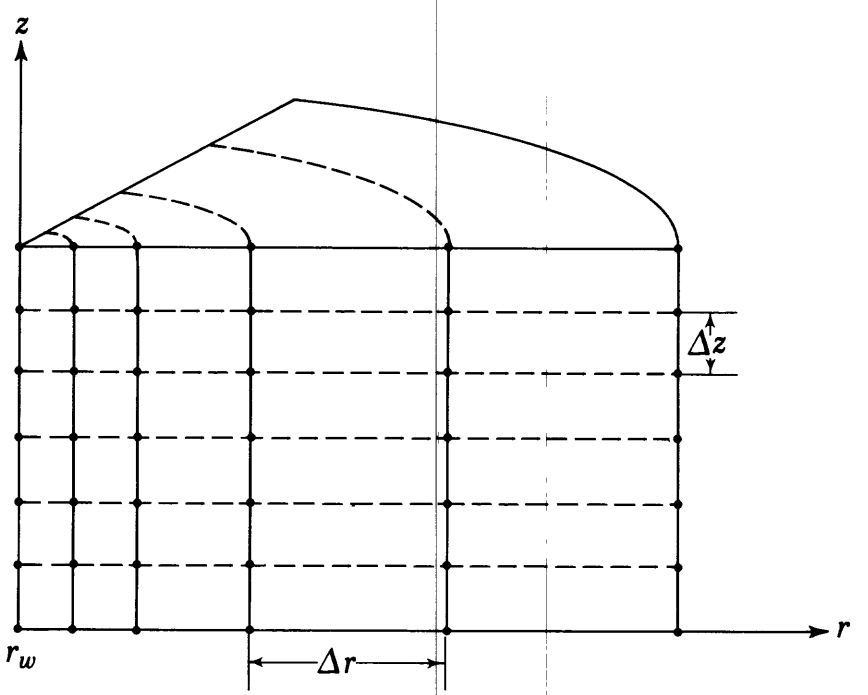

Figure 8 - Node array in the r-z plane

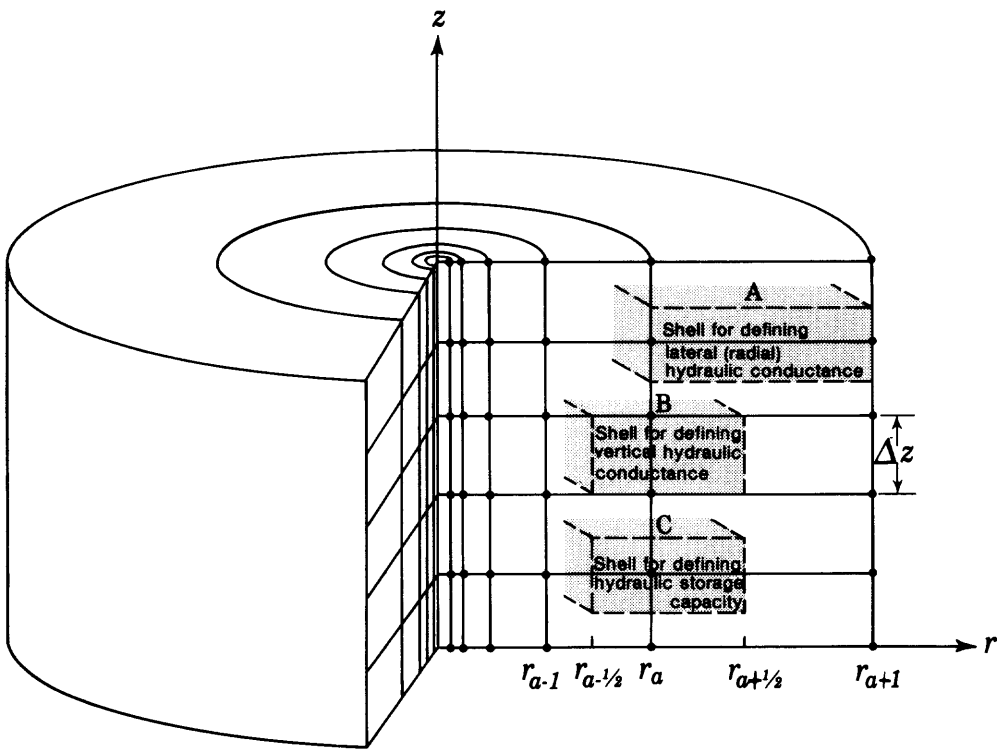

Figure 9 - Shells used for definition of hydraulic conductance and storage capacity in axially symmetric flow

Lateral Conductance

By virtue of our assumption of a uniform vertical mesh spacing, the thickness of shell A turns out to be equal to the vertical spacing, Δz. Thus, the lateral conductance of shell A can be calculated using equation (9), taking the thickness as Δz rather than b. In the following problem, we take the outer radius, r_{a+1}, to be twice the inner radius, r_a, the log term is simply ln 2. For the problem, therefore, equation (9) becomes

$$C_r = \frac{2\pi K_L \Delta z}{\ln 2} = \frac{2\pi K_L \Delta z}{0.693} \qquad (13)$$

where K_L represents lateral hydraulic conductivity. Note that because the ratio $\frac{r_{a+1}}{r_a}$ is constant throughout the model mesh, this expression remains the same for all lateral conductances along any given row (differences between rows may arise due to variation in the term K_L from one row to another, if layers of different hydraulic conductivity are simulated.)

Finally, it should be noted that along the upper row of the mesh of figure 9, the lateral hydraulic conductance values are not based on a full-thickness shell such as A, but rather of a shell of half thickness, $\Delta z/2$, which extends downward from the row but not above it. Similarly, along the lower row of the mesh, lateral hydraulic conductance values are based on a shell which extends upward from the row but not below it, and again the thickness used in calculation is $\Delta z/2$.

Vertical Conductance

The vertical conductance of shell B in figure 9 can be calculated as the product of the vertical hydraulic conductivity and cross sectional area of flow, divided by the distance of flow, $(K_z A/\Delta z)$. Figure 10 shows an isolated view of shell B. Because we are dealing with vertical velocity components, the cross-sectional area of flow is the area of the upper surface of the shell--that is, the shaded annular area of figure 10. As shown in figure 9, shell B extends vertically between two nodes of the model mesh; these nodes fall on the vertical column located at radius r_a. This radius, r_a, is indicated by the dashed circle in figure 10. The cross sectional area of flow extends inward from r_a to an interior radius, $r_{a-1/2}$, and outward from r_a to an outer radius $r_{a+1/2}$. The total area of flow is the difference between the area of a circle of radius $r_{a+1/2}$ and the area of a circle of radius $r_{a-1/2}$. Thus the area of flow is given by

$$A = \pi[(r_{a+1/2})^2 - (r_{a-1/2})^2].$$

Figure 11 shows a plan view of the cross-sectional area of flow, again with r_a indicated by a dashed circle. The area has been divided into two segments: A_1, which is interior to r_a, and A_2, which is exterior to r_a. We wish to choose the inner and outer radii, $r_{a-1/2}$ and $r_{a+1/2}$, in such a way that the vertical hydraulic conductance between two nodes will be distributed evenly, half outside the radius of the node, and half inside that radius. This is achieved by making the two areas A_1 and A_2 equal. For the radial node spacing of our problem, in which each node falls at a radius which is twice that of the node interior to it, the radii $r_{a-1/2}$ and $r_{a+1/2}$ must be given by

$$r_{a-1/2} = r_a\sqrt{2/5} \tag{14}$$

$$r_{a+1/2} = r_a\sqrt{8/5} \tag{15}$$

in order for the areas A_1 and A_2 to be equal.

Exercise 4: verify that for any value of r_a, the area between $r_a\sqrt{2/5}$ and r_a is equal to the area between r_a and $r_a\sqrt{8/5}$.

Using equations (14) and (15), the cross sectional area for vertical flow is given by

$$A = \pi\{(r_a\sqrt{8/5})^2-(r_a\sqrt{2/5})^2\} = \frac{6\pi r_a^2}{5} \tag{16}$$

The vertical hydraulic conductance of shell B is thus given by

$$C_z = \frac{K_z A}{L} = \frac{K_z(6\pi/5)r_a^2}{\Delta z} = \frac{3.77K_z r_a^2}{\Delta z} \tag{17}$$

where K_z is the hydraulic conductivity in the vertical direction.

[Note: These results hold only if we are using $\frac{r_{a+1}}{r_a} = 2$ in our model design. More generally, if $\frac{r_{a+1}}{r_a} = \alpha$, and if we wish to have an equal distribution of area outside and interior to the node, then the area must be taken from an inner radius of $r_a[2/(\alpha^2+1)]^{1/2}$ to an outer radius of $\alpha r_a[2/(\alpha^2+1)]^{1/2}$. The area of vertical flow then becomes $2\pi\{\frac{\alpha^2-1}{\alpha^2+1}\}r_a^2$.]

From equation (17), the vertical conductance of shell B is seen to be the product of a constant term, $\frac{3.77K_z}{\Delta z}$, and the square of the radius around

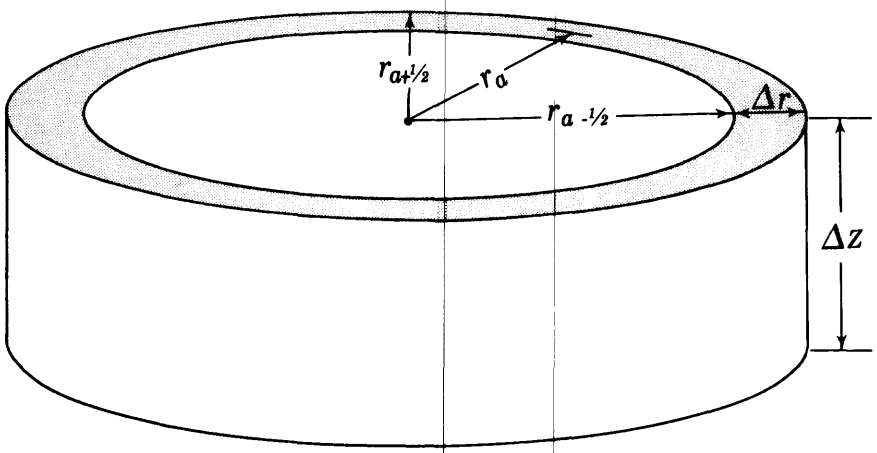

Figure 10 - Cylindrical shell extending inward and outward from the node column at radius r_a

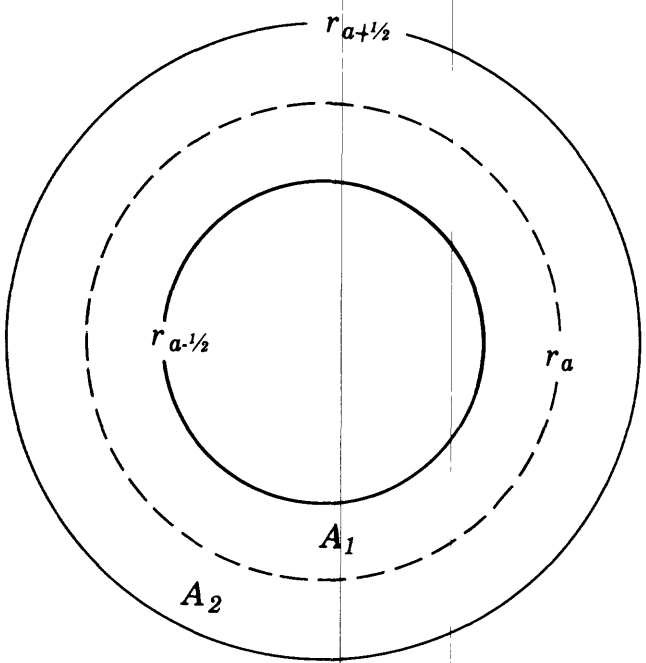

Figure 11 - Top view of cylindrical shell extending inward and outward from the node column at radius r_a

which the shell is centered. If we are calculating the vertical hydraulic conductance of successive shells, moving radially outward along a model row, the conductance of each shell will be four times that of the shell interior to it, since the radius of each shell is twice that of the shell interior to it. (Again, this holds only for $\frac{r_{a+1}}{r_a} = 2$; for the more general case, $\frac{r_{a+1}}{r_a} = \alpha$, the conductance of each shell would be α^2 times that of the shell interior to it. In any case, if the vertical hydraulic conductance of a single shell is determined, that of successive shells along the same model row can be obtained readily; however, differences between rows will arise if different values of K_z are incorporated, simulating layers of different hydraulic conductivity.)

Finally, it should be noted that along the inner vertical column of nodes in the mesh of figure 9 (i.e., the column along r_w) vertical hydraulic conductance values are based on a cylindrical shell which extends radially outward from r_w but not interior to it. This shell thus has half the base area, and half the vertical conductance which a full shell at the same radius would have. Similarly, along the outer vertical column of nodes (i.e., the column along r_e), conductance values are based on a shell which extends inward from r_e but not beyond it. Again, area of flow and the vertical conductance are half those of a full shell at the same radius.

Storage Capacity

Unlike shells A and B in figure 9, which are taken between two nodes for the purpose of calculating hydraulic conductance, shell C is distributed around a single node, and is used to illustrate the calculation of storage capacity associated with that node. The storage capacity of the shell is the specific storage multiplied by the volume of the shell; the shell volume, in turn, is simply the base area of the shell multiplied by its thickness. The shell extends vertically halfway to the adjacent nodes above and below; since we are assuming an even mesh spacing, the thickness is simply Δz, like that of shell A. The node around which shell C is centered is located at a radius r_a--i.e., it lies on the same vertical column as the nodes of shell B. Like shell B, shell C extends outward to a radius $r_{a+1/2}$, or $r_a\sqrt{8/5}$, and inward to a radius $r_{a-1/2}$ or $r_a\sqrt{2/5}$. Thus, it has the same base area as shell B--the area given by equation (16). Moreover, as shown for shell B, the base area of the section of shell C beyond r_a is equal to base area of the section interior to r_a. The volumes of these two sections are therefore equal, and it follows that the storage capacity of the section beyond r_a will equal that of the section interior to r_a. In other words, storage capacity is evenly distributed around r_a.

The base area of shell C, as given by equation (16) is $6\pi r_a^2/5$; the hydraulic storage capacity, which is simply the product of specific storage and volume, is therefore given by

$$SC = \frac{6\pi S' \Delta z}{5} r_a^2 \qquad (18)$$

where S' is the specific storage of the aquifer material. As with vertical hydraulic conductance, therefore, the storage capacity of a shell centered at r_a is given by the product of a constant and r_a^2. Moving outward along a row, the storage capacity of each successive shell will be four times that of the shell interior to it, since the radius at each node is twice that at the node interior to it. Thus, again when one storage capacity is determined along a given row, the remainder can be calculated very quickly.

Shell C is distributed vertically in the same way as shell A, and radially in the same way as shell B. It follows that the adjustments which we had to make along the upper and lower rows for shell A must also be applied here, and the adjustments which we made along the inner and outer columns for shell B must similarly be applied. Along these boundaries, the shells used to define storage capacity have only half the volume of shells in the interior of the mesh, and the storage capacities must accordingly be cut in half; for "corner nodes", which fall on both a row boundary and a column boundary, storage capacity must be reduced to one quarter of the value for an interior node.

A further consideration enters if the model is used to represent an unconfined aquifer, and the uppermost row of the mesh is taken as the water table. In these cases, the storage capacity associated with nodes along the uppermost row must account for the effects of unconfined storage. Thus for nodes in the top row, in a water table simulation, storage capacity is taken as the product of specific yield, S_y, and the base area of the shell, $(6\pi r_a^2)/5$. Other modifications of the model to represent a water-table situation might include some provision for adjusting the lateral conductance of nodes at the top of the mesh, as water levels fall, and for removing "dewatered" nodes from the model; these topics are beyond the scope of the present discussion.

RADIAL-FLOW PROBLEM

The problem which we will undertake in this section consists of two parts. In the first, we will design a model for the analysis of radial flow to a well; second, we use some results from the model to construct a flow net. We will observe how the simulated results may be used to calculate certain characteristics of the flow regime. It is important to keep in mind the internal characteristics and boundary conditions of any radial flow model because these factors determine how well the mathematical representation approximates the real system under study.

Model Design

Figure 12 shows a partially penetrating well in a semi-confined aquifer. The confining unit is 100 feet thick and is overlain by a water-table aquifer in which heads may be considered constant. The hydraulic conductivity of the confining unit, in both the lateral and vertical directions, is 0.1 gallon per day square foot. The specific storage of the confining unit may be considered zero. The aquifer is 100 feet thick, its lateral hydraulic conductivity is 100 gallons per day per square foot, and its anisotropy (ratio of lateral to vertical hydraulic conductivity) is 100. The specific storage of the aquifer is 10^{-6} per foot. The discharging well is screened from 30 to 70 feet below the top of the aquifer; the screen radius is 1 foot. Water levels throughout the system prior to pumping are 100 feet above datum (which is the top of the confining unit), and remain at this level in the overlying water-table aquifer throughout pumping.

The well is pumped at a rate of 250,000 gallons per day; we assume this pumpage to be uniformly distributed along the well screen. We wish to know how long it will take for the system to reach equilibrium, and we require the head distribution and the stream function distribution, as functions of r and z, at this new equilibrium. (Stream functions are discussed in part B of this section.)

We wish to design a digital model which will provide the head distribution as a function of r, z, and time. We will use a vertical mesh specing of 50 feet in the confining unit and 20 feet in the aquifer. In the radial direction, we will let $r_{n+1}/r_n = 2$, where r_n is the radius represented by a given node, and r_{n+1} is that represented by the succeeding node along the r axis. We assume that the effect of the well at equilibrium will not extend beyond 30,000 feet from the discharging well and we will define a vertical no-flow boundary at that distance.

Figure 13 shows the array of nodes in the r-z plane which will make up our model, superposed on the hydrologic features of figure 12. The column number, J, of each column is indicated across the top of the array while the row number, I, of each row is indicated along the left margin. Using figure 13 do the following parts of the problem:

1. The radii associated with columns 1 and 16 are shown beneath the column number of figure 13; enter the radii associated with each of the remaining columns.

2. The depth (below the top of the confining bed) associated with rows 1, 2, 3, and 8 is shown on the left side of figure 13, to the right of the row number; enter the depths associated with the remaining rows.

3. Along the right margin of figure 13, division marks have been placed representing the depths midway between successive horizontal rows of nodes. Enter the depth (below the top of the confining bed) represented by each of these marks.

4. Blocks A, B, C, D, E, F, and G in figure 13 represent some of the aquifer volume elements for which lateral hydraulic conductance must be

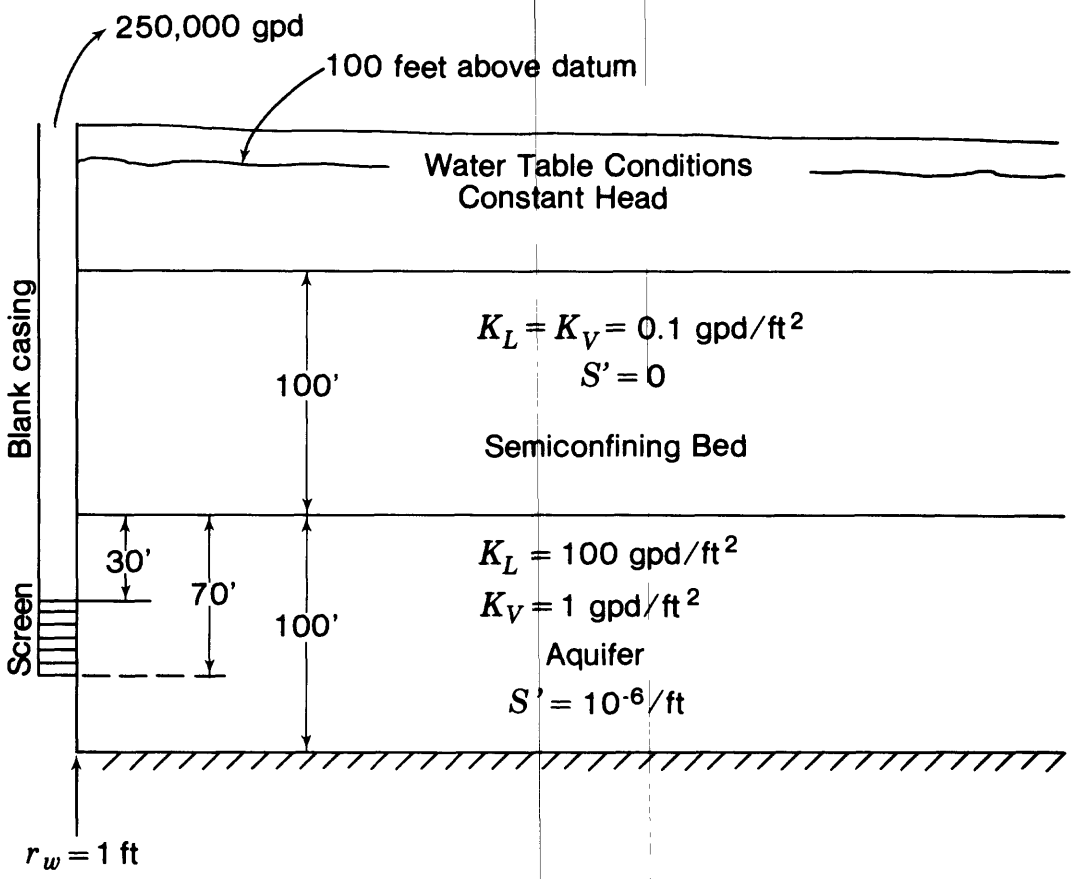

Figure 12 - Schematic of hydrologic conditions for the radial flow problem

specified in the model; that is, each of these rectangular blocks represents a vertical cross section through one of these three-dimensional volume elements. What is the geometric form of these elements?

5. Calculate the lateral hydraulic conductance of the volume element represented by each of the blocks A through G of figure 13. In the case where the volume element is composed of two layers of differing hydraulic conductivity parallel to the direction of flow, the total hydraulic conductance is simply the sum of the two individual lateral conductances. (The general rule is that an equivalent conductance for conductances in parallel is the sum whereas an equivalent conductance for conductances in series is calculated by equation 11 as discussed previously).

6. To prepare for the calculation of vertical conductances, we divide the aquifer into shells around each node, such that each shell extends from an inner radius $r\sqrt{2/5}$ to an outer radius $r\sqrt{8/5}$, where r is the radius represented by the node. The vertical marks along the lower margin of figure 13 represent these lines of division. The radius associated with the division mark between nodes 1 and 2, and that associated with the division between nodes 15 and 16, is shown on figure 13. Enter the radii associated with each of the remaining division marks.

7. If we project these division marks to the surface (that is, to a map view of the aquifer, each mark will trace a circle on that surface. The area between two successive circles will then represent the base area of a cylindrical shell. This area has been calculated for the interval around column 15, and the results are shown between the appropriate division marks at the bottom of figure 13. Enter the area for each of the remaining intervals. (Note that the interval "around" column 1 does not extend inward from column 1, and that the interval "around" column 16 does not extend outward beyond column 16.)

8. Blocks H and I on figure 13 represent volume elements, or shells, for which vertical hydraulic conductance must be calculated. Each of these elements extends vertically between rows 4 and 5 of the mesh. Working across this interval between rows 4 and 5, sketch the outlines of the remaining blocks for which vertical hydraulic conductance must be specified (i.e., sketch these blocks directly on figure 13; do this only for the interval between rows 4 and 5). Calculate the vertical hydraulic conductance of the volume elements represented by the four innermost blocks (i.e., those closest to r_w) and by the three outermost blocks (those at columns 14, 15, and 16). Indicate your results on the figure.

9. Blocks J and K on figure 13 represent volume elements, or shells, for which storage capacity must be calculated. Each of these blocks is centered around a node in row 7 of the mesh. Sketch the outlines of the remaining blocks in row 7 for which storage capacity must be specified (i.e., sketch these blocks directly on figure 13). Calculate the storage capacities of the volume elements represented by the four innermost blocks (closest to r_w) and by the three outermost blocks. Repeat these calculations for the blocks directly underlying these, in row 8. Calculate the amount of water released by a 1-foot drop in head in the block at row 7, column 16.

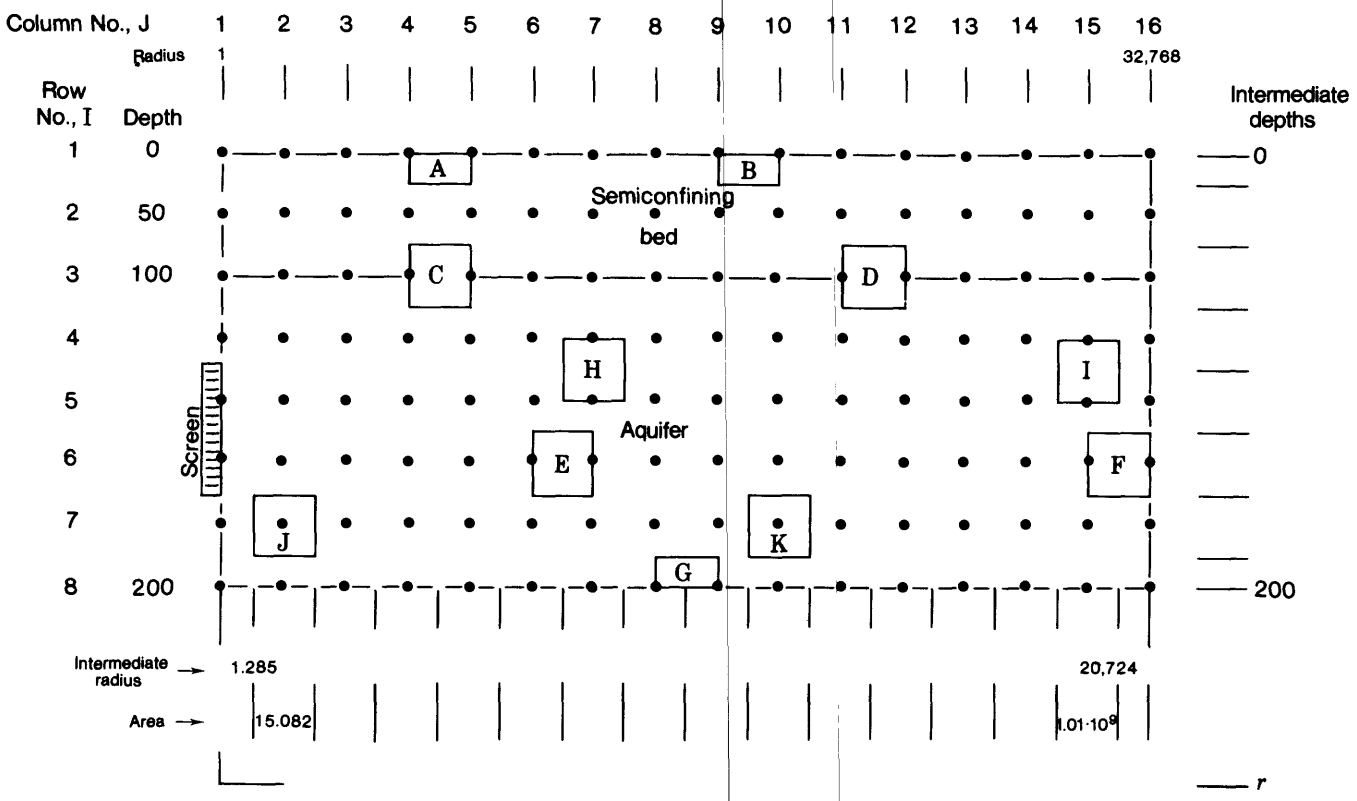

Figure 13 - Model node array and volume elements used in calculating simulation coefficients

10. On figure 13, indicate the nodes which are to be held at constant head, and those which represent the well screen. Indicate the discharge which must be withdrawn through each node representing the screen.

Stream Functions

Before proceeding to the second part of our problem, we will review the concept of stream function.

In two-dimensional flow, streamlines or flowlines are lines within a flow system to which the velocity vectors are everywhere tangent at a particular instant of time. The fact that the velocity vectors are everywhere tangential to the streamlines means that no flow can cross a streamline. In a steady state problem, where the characteristics of the flow regime do not change with time, the streamlines remain the same at all times; in this situation, each streamline represents a fixed line within the system across which there is never any flow. If we consider two streamlines extending completely through the flow regime, the region between these lines is called a stream tube. Since flow cannot cross either bounding streamline, the flow through a stream tube is the same at any cross section along the length of the stream tube. In this sense, a stream tube in a steady-state flow may be thought of as a pipe or conduit extending through the flow system, always carrying the same fraction of the total flow.

In a three-dimensional problem, we must deal with three-dimensional stream surfaces rather than two-dimensional streamlines. Figure 14 shows the flownet of figure 7 with some additional quantities identified. The flowlines shown in figure 14 actually represent the lines of intersection of three-dimensional stream surfaces with the vertical r-z plane; and the areas between streamlines represent the intersection of three-dimensional stream tubes with the r-z plane. Again, however, the axial symmetry of the radial flow regime allows us to treat the problem in a two-dimensional analysis, even though we are actually dealing with three-dimensional features.

The nine streamlines shown on figure 14 divide the flow regime into 10 stream tubes; the flowlines were constructed in such a way that the flow carried in each of these stream tubes is 10 percent of the total flow moving through the system. Each streamline has been labelled with a number which gives the fraction of the total flow occurring above and interior to that streamline; for example, the deepest streamline shown on the figure is labelled 0.9, indicating that nine-tenths of the flow occurs above (i.e., interior to) this line, whereas one-tenth occurs below (i.e., outside of) this line. These fractions labelling the various flowlines are termed stream functions. They are constant along a streamline because no flow crosses from one side of a steamline to the other. Thus, we may look at the streamlines as contours of the stream function values; and it follows that if we can devise some way of calculating stream function values, and can then contour the results, we can construct the streamlines corresponding to these stream function values.

In figure 14, the 1.0 streamline follows the right margin of the flownet at r_e, the bottom of the flow net along the base of the aquifer, and the left margin of the flow net at r_w beneath the well screen; 100 percent of the flow occurs above and interior to this line. The 0.0 streamline

follows the vertical at r_w between the top of the screen and the water table; no flow occurs interior to this line. All of the streamlines intersect the upper surface of the flow net, representing the water table, since the system is one in which the flow is sustained by uniform areal recharge to the water table. Thus, for example, the stream tube between the 0.8 and 0.9 streamlines begins at the water table, where it covers an area sufficient to intercept 10 percent of the total recharge, and extends to the lower part of the well screen; it may be thought of as the conduit through which that particular fraction of the recharge reaches the well.

Stream functions exhibit a number of interesting and useful analytical properties; discussions of these can be found in most standard texts in fluid mechanics. In general, stream functions are defined for two-dimensional flow systems and for axially symmetric three-dimensional systems such as the one we are considering. In terms of ground-water flow, at least, the use of stream functions is restricted to steady-state problems. In transient ground-water problems, we must assume that water is being released from compressive storage at points in the interior of the flow; thus, even if streamlines can be defined, the fraction of the total flow between any two streamlines will generally vary from one point to another, and we cannot assign fractions to each streamline which will describe the flow above (i.e., to one side of) that streamline.

Flow-net Construction

Figure 15 represents the node array for the model we designed in the first part of this exercise; the dashed lines outline the lateral conductance blocks (or shells) for the entire mesh. Referring back to figure 12, the problem stated that the semiconfining unit was overlain by a water-table aquifer in which head remained constant; this was accommodated in the model design by holding the head constant in the nodes along the top row of the mesh. These nodes thus constitute the recharge points for the model. Recharge entering at, say, the top node in column 15 will distribute itself in some way along the nodes of column 15 by vertical flow; however, none of the flow entering column 15 can reach the nodes of column 14 except through the lateral conductances between those two columns. It follows that we can account for all of the flow past any vertical line through our model by considering lateral movement alone; we will use this concept in the calculation of stream functions.

Figure 16 again shows the node array of our model, but now with a value of head associated with each node. These head values were obtained by running a simulation, using the model as we designed it, for 20 time steps; the length of the first time step was taken as 0.001 day, and the length of each subsequent step was twice that of the step preceding it. Using this scheme, the end of the twentieth step corresponded to a time of 1048 days. The well discharge was simulated as 250,000 gallons per day. At the end of 20 time steps, the head distribution was no longer changing with time, and withdrawal of water from storage in the mesh was negligible; thus, steady-state conditions had been reached, and the pumpage was being supplied by recharge from the constant head nodes along the upper boundary. Under these conditions, the streamlines are unchanging with time, and construction of a flow net can provide a gread deal of useful information about the system.

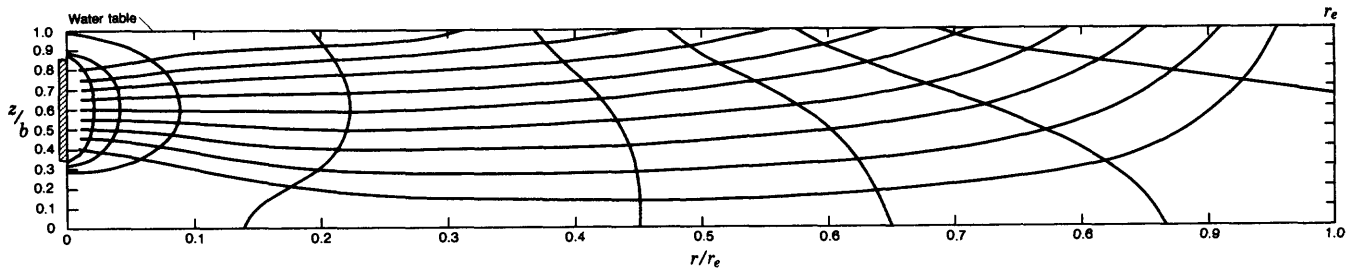

Figure 14 - Flow net in the r-z plane for axially symmetric flow to a well. Stream-function values are shown for each streamline and relative head values (as a percentage of maximum head difference) are shown for each line of equal head.

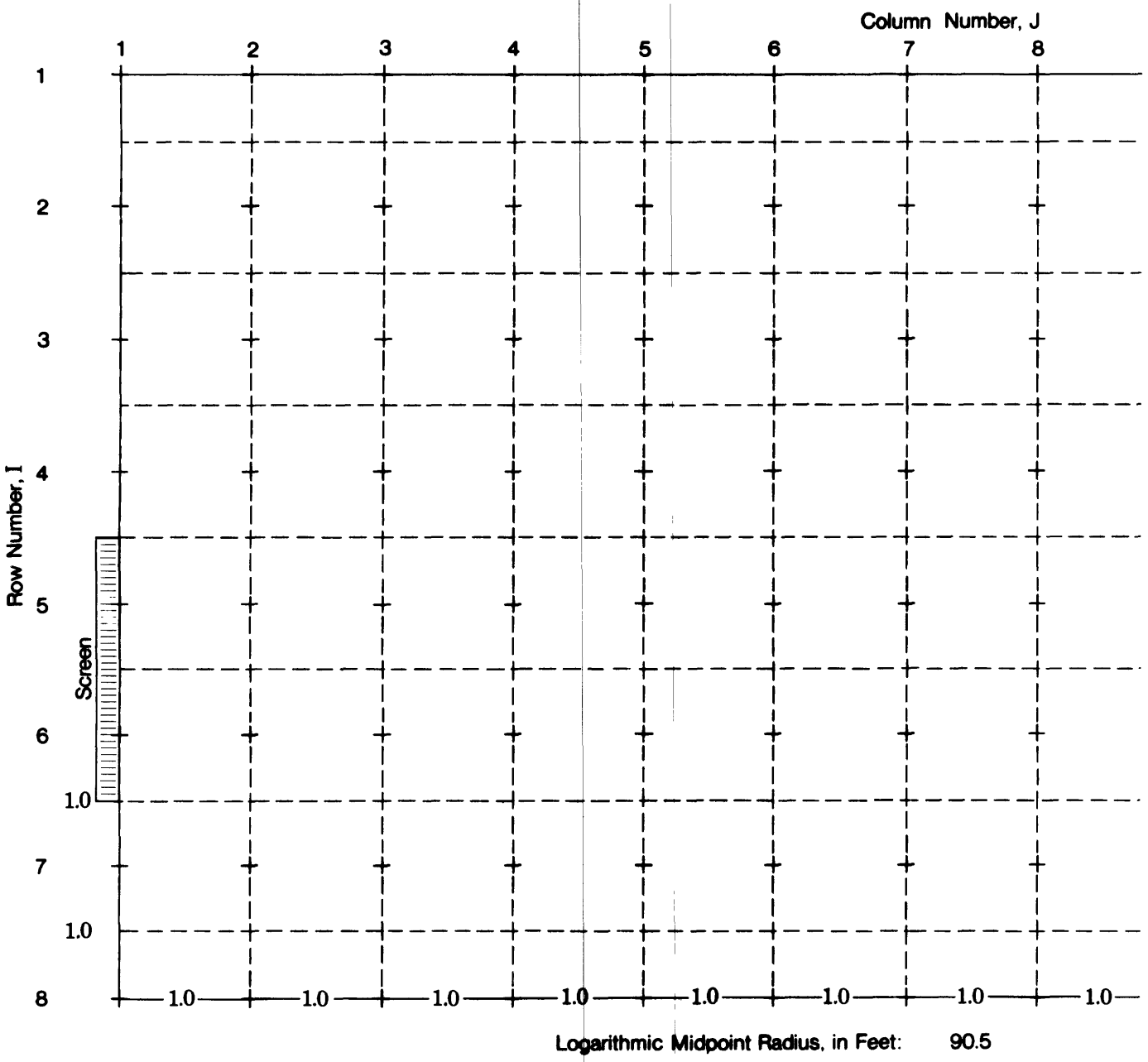

Figure 15 - Node array and lateral hydraulic conductance blocks

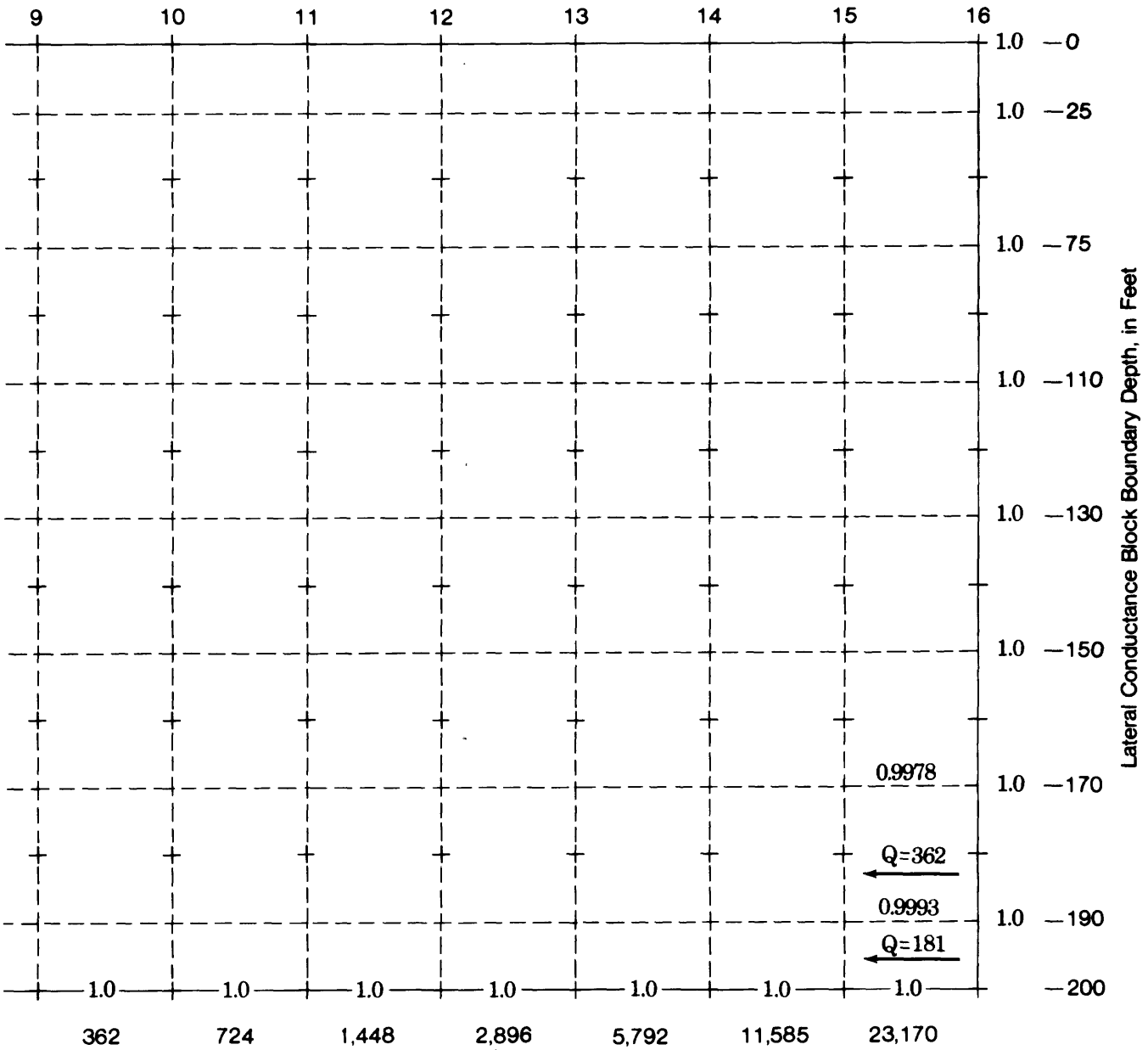

for stream function calculation

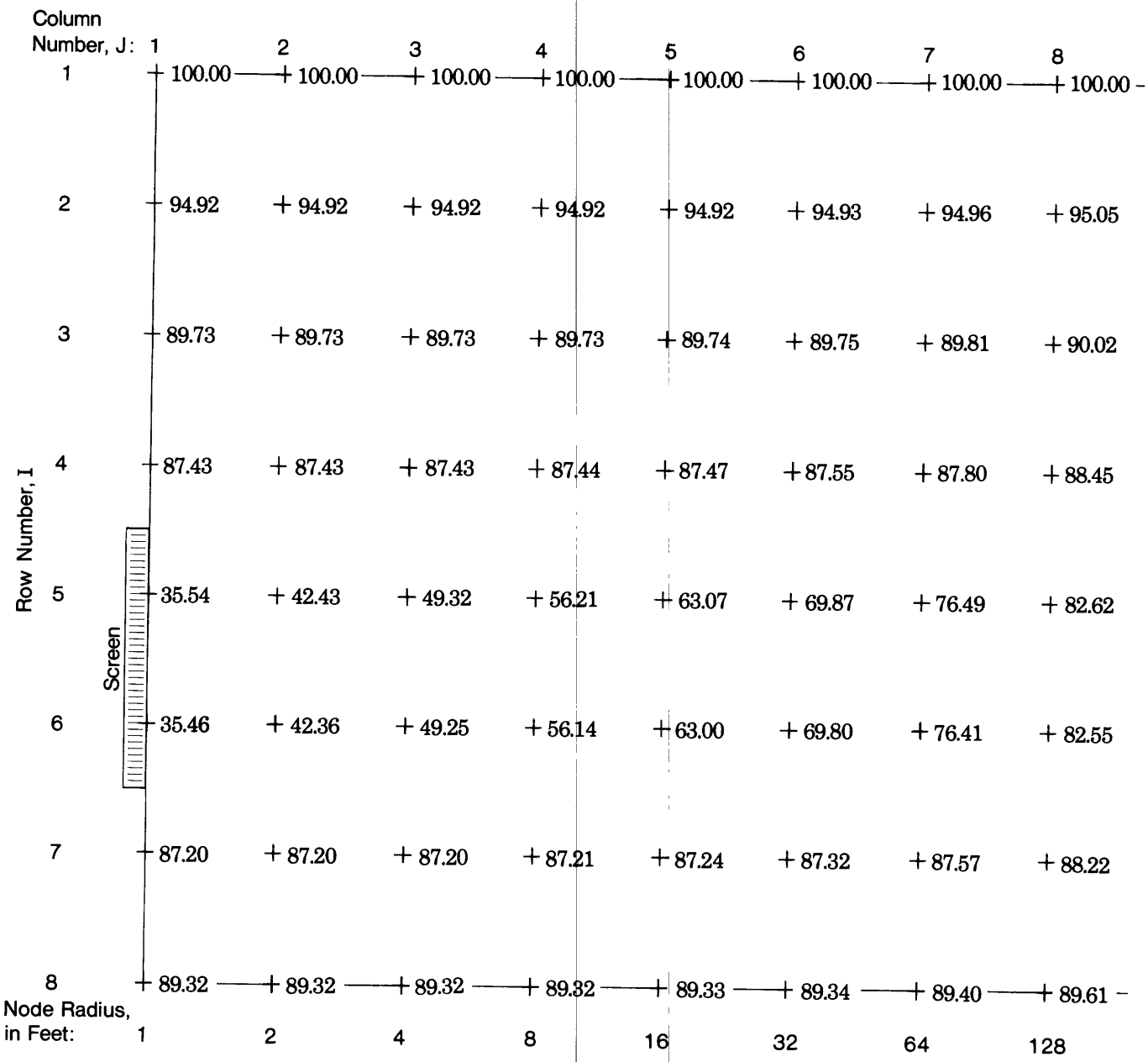

Figure 16 - Node array showing head values

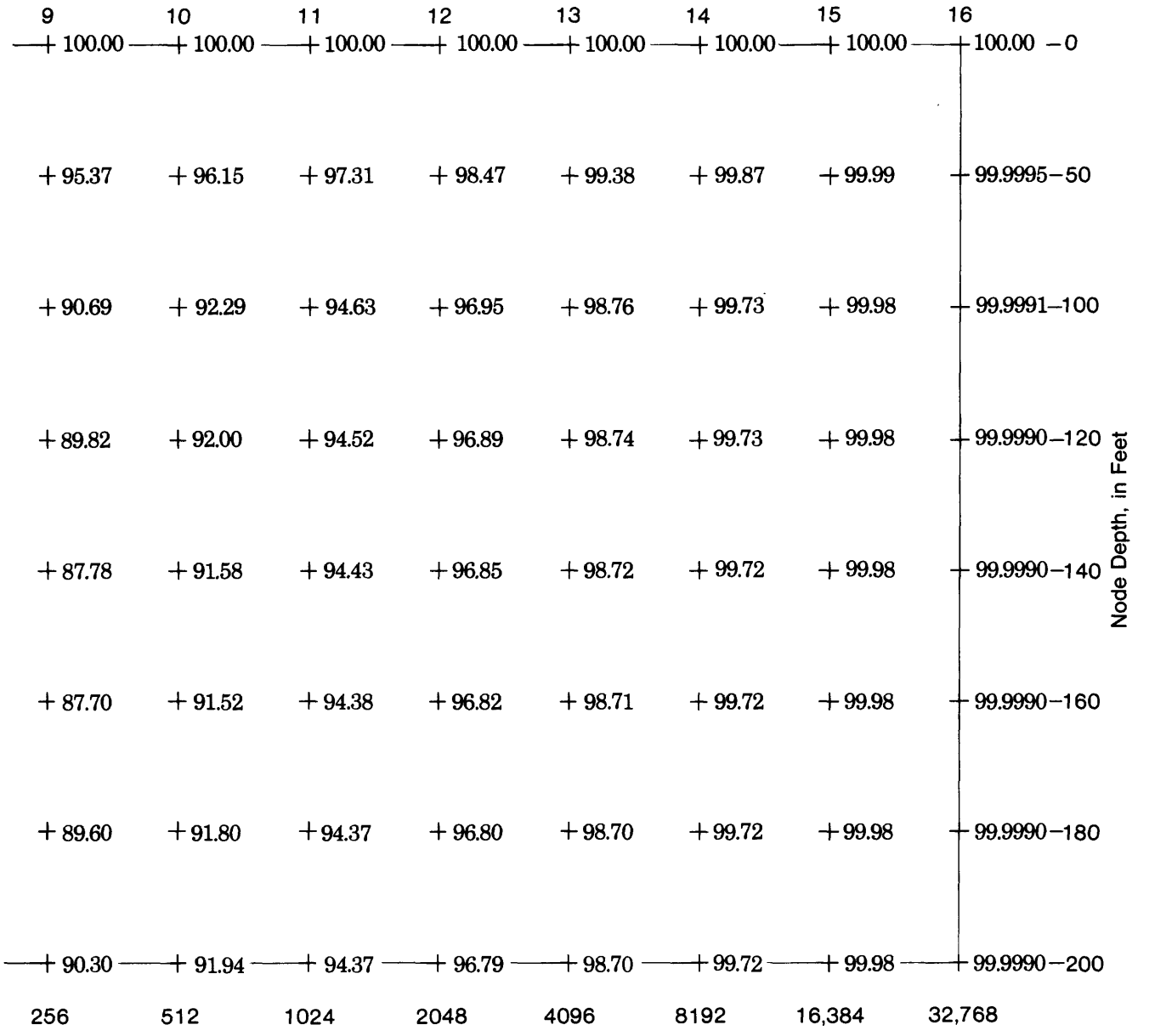
9
10
11
12
13
14
15
16
100.00 100.00 100.00 100.00 100.00 100.00 100.00 100.00 −0
95.37 96.15 97.31 98.47 99.38 99.87 99.99 99.9995−50
90.69 92.29 94.63 96.95 98.76 99.73 99.98 99.9991−100
89.82 92.00 94.52 96.89 98.74 99.73 99.98 99.9990−120
87.78 91.58 94.43 96.85 98.72 99.72 99.98 99.9990−140
87.70 91.52 94.38 96.82 98.71 99.72 99.98 99.9990−160
89.60 91.80 94.37 96.80 98.70 99.72 99.98 99.9990−180
90.30 91.94 94.37 96.79 98.70 99.72 99.98 99.9990−200
256
512
1024
2048
4096
8192
16,384
32,768
Node Depth, in Feet

The heads shown on figure 16 allow us to calculate the flow through any lateral conductance in the mesh, simply by multiplying the head difference across the conductance by the value of the conductance. We will use the diagram of figure 15 as a worksheet for our analysis. We begin by noting stream function values along r_e (column 16), along the base of the aquifer (row 8), and along r_w (column 1) beneath the screen. As we have seen, the stream function must be 1.0 on this perimeter; this value has already been entered on figure 15. Next, we focus on the conductance block in the lower right-hand corner of the mesh--that is, the lowermost block extending between column 16 and column 15. Using the head values from figure 16, we calculate the flow through this block. Because the difference in head across the block is 0.02 feet and the conductance is 9067 gpd/ft (which was calculated in part 5 of the problem previously), we find the flow to be approximately 181 gpd. Now we calculate the fraction of the total flow this represents. The total flow through the system is just the well discharge, 250,000 gpd; so we divide the flow through our conductance block by 250,000, and see that it represents about 0.0007, or 0.07 percent, of the flow through the system. At the bottom of the conductance block, along the base of the aquifer, the stream function value is 1.0, indicating that 100 percent of the flow occurs above or interior to that point. If 0.07 percent of the flow occurs through the block, 99.93 percent must occur above and interior to the upper surface of the block. So the stream function at the top of the conductance block must be 0.9993. This value is already entered on figure 15, midway between columns 16 and 15, at the top of the lowermost conductance block.

Next, we move upward to the conductance block immediately above the one we have just considered. Again, we calculate the flow; since the conductance here is double that for the lower block, and the head difference is almost the same, the flow through this block turns out to be approximately twice that through the lower one, or 363 gpd. Again, we divide by 250,000 to find that this represents about 0.15 percent of the total flow. Thus, since the stream function at the base of this block was 0.9993, and 0.15 percent (0.0015) of the flow passes through the block, we find by subtraction that the stream function at the upper surface of the block must be 0.9978. This also has been entered already on figure 15, and on the worksheet for the calculation of stream functions (table 2). Using the worksheet, continue working upward in this manner through the "stack" of conductance blocks between columns 15 and 16, calculating the fraction of total discharge through each block and subtracting this from the stream function value at the base of the block to find the stream function at the top of the block. Enter these values on figure 15 at the top of each block, midway between the nodes. Then move over to the stack of conductance blocks between columns 15 and 14 and repeat the procedure, again beginning with the bottom block and working up. Note that the stream function value at the bottom of the lowermost block is again 1.0, so that we must begin the series of calculations by subtracting from 1.0 again, as we did in the initial series. After each calculation, enter the stream function value at the top of the block, midway between the node columns. Repeat this procedure for the intervals between columns 14 and 13, 13 and 12, 12 and 11, 11 and 10, 10 and 9, and finally for the interval between columns 7 and 8. Note that many of the calculations have been computed for you on the worksheet (table 2).

The procedure of calculation which we have used can be described formally through the equations

$$Q_{I,J} = CX_{I,J}(H_{I,J+1} - H_{I,J}) \tag{18}$$

and

$$\Psi_{I,J} = 1.0 - \sum_{n=I}^{n=NR} \left(\frac{Q_{n,J}}{Q_w}\right) \tag{19}$$

where $Q_{I,J}$ is the flow through the lateral conductance block between node I,J and node I,J+1; $CX_{I,J}$ is the value of lateral hydraulic conductance for this block; $H_{I,J}$ and $H_{I,J+1}$ are the head values at nodes I,J and I,J+1, respectively; $\Psi_{I,J}$ is the stream function at the top of the conductance block between I,J and I,J+1; Q_w is the well discharge--that is, the total flow through the system; and NR is the total number of rows in the model, so that the summation of equation (19) includes the flow through the lateral conductance between node I,J and node I,J+1, and the flow through all of the lateral conductances vertically below this in the stack.

Now go back and interpolate within each vertical "stack" of stream function values to locate the positions of the 0.9, 0.8, 0.7, 0.6, 0.5, 0.4, 0.3, 0.2, and 0.1 stream function values within each stack. Note that all of these values will not be present in every stack; in terms of the diagram of fig. 14, the streamlines must intersect the upper constant-head boundary of the model, illustrating accretion due to recharge. Thus, for example, the 0.2 stream function does not appear in the outer part of the mesh, toward r_e. Note also that as we approach the well screen, the flow tends to be compressed into the screened interval; in terms of the model, this means that most of the flow will ultimately be squeezed into the lateral conductance blocks in the two rows which lead to the screen. Thus, toward the left side of the model mesh (toward r_w), virtually all of the interpolated stream function values will fall within the lateral conductance blocks for rows 5 and 6 of the model.

Figure 15, because it represents the model mesh, has a logarithmic scale along the radial axis; to construct our flownet, we wish to transfer our values to an arithmetic scale diagram. Before doing this, we must decide at what points in the r-z plane our stream function values are to be plotted. To assign vertical coordinates, remember that in our method of calculation, we tacitly assumed that the vertical coordinate of each calculated stream function value was at the top of the conductance block through which flow was computed. We assigned vertical coordinates to the interpolated values through the process of vertical interpolation itself. To assign radial coordinates, we make the assumption that the radial coordinate of each stream function value falls at the logarithmic midpoint of the conductance block through which flow was calculated--i.e., that for a conductance block extending from an inner radius of r_j to an outer radius of $2r_j$, the calculated stream function values actually apply at a radius of $\sqrt{2}\, r_j$. This actually represents an assumption that our stream function values apply at a radius which "bisects" the lateral conductance, in the sense that the lateral conductance between r_j and $\sqrt{2}\, r_j$ is equal to that between $\sqrt{2}\, r_j$ and $2r_j$. Values of these logarithmic midpoint radii are shown below the r axis on

Table 2 - Work Sheet for the Calculation of Stream Functions

Between columns	Row	Head Drop Between Columns Δh (ft)	Lateral Hydraulic Conductance C_L (gpd/ft)	Flow through Conductance Block Q (gpd)	Cumulative Flow ΣQ (gpd)	Stream-Function Value $1 - \frac{\Sigma Q}{Q_T}$ (unitless)
15 & 16	8	0.02	9,067	181	181	0.9993
	7	0.02	18,130	363	544	0.9978
	6					
	5					
	4					
	3					
	2					
	1					
14 & 15	8					
	7	0.26				
	6	0.26	18,130	4,714		
	5	0.26	18,130	4,714		
	4	0.25	18,130	4,532		
	3	0.25	9,090	2,272		
	2	0.12	45.4	5		
	1	0	22.7	0		
13 & 14	8	1.02	9,067	9,248	9,248	0.9630
	7	1.02	18,130	18,490	27,738	0.8890
	6	1.01	18,130	18,310	46,048	0.8158
	5	1.00	18,130	18,130	64,178	0.7433
	4	0.99	18,130	17,950	82,128	0.6715
	3	0.97	9,090	8,817	90,945	0.6362
	2	0.49	45.4	22	90,967	0.6361
	1	0	22.7	0	90,967	0.6361
12 & 13	8	1.91	9,067	17,318	17,318	0.9307
	7	1.90	18,130	34,450	51,768	0.7929
	6	1.89	18,130	34,270	86,038	0.6558
	5	1.87	18,130	33,900	119,938	0.5202
	4	1.85	18,130	33,540	153,478	0.3861
	3	1.81	9,090	16,453	169,931	0.3203
	2	0.91	45.4	41	169,972	0.3201
	1	0	22.7	0	169,972	0.3201

Work Sheet for the Calculation of Stream Functions (continued)

Between columns	Row	Head Drop Between Columns Δh (ft)	Lateral Hydraulic Conductance C_L (gpd/ft)	Flow Through Conductance Q (gpd)	Cumulative Flow ΣQ (gpd)	Stream-Function Value $1 - \frac{\Sigma Q}{Q_T}$ (unitless)
11 & 12	8	2.42	9,067	21,942	21,942	0.9122
	7	2.43	18,130	44,060	66,002	0.7360
	6	2.44	18,130	44,240	110,242	0.5590
	5	2.42	18,130	43,870	154,112	0.3836
	4	2.37	18,130	43,000	197,112	0.2116
	3	2.32	9,090	21,089	218,201	0.1272
	2	1.16	45.4	53	218,254	0.1270
	1	0	22.7	0	218,254	0.1270
10 & 11	8	2.43	9,067	22,032	22,085	0.9117
	7	2.57	18,130	46,590	68,675	0.7253
	6					
	5					
	4	2.52				
	3	2.34				
	2	1.16				
	1	0				
9 & 10	8	1.64	9,067	14,870	14,870	0.9405
	7	2.20	18,130	39,890	54,760	0.7810
	6					
	5					
	4	2.18				
	3	1.60				
	2	0.78				
	1	0				
7 & 8	8	0.21	9,067	1,904	1,904	0.9999
	7	0.65	18,130	11,780	13,684	0.9453
	6					
	5					
	4	0.65				
	3	0.21				
	2	0.09				
	1	0				

figure 15, for each stack of lateral conductance blocks used in our stream function calculations. In setting up an arithmetic flownet plot, we will use an exaggerated vertical scale, and it will be an advantage to use a reasonably large field--for example, a scale of 20 feet to the inch on the vertical axis and 500 feet to the inch on the radial axis. The well should be at the left side of your figure. The flow net need not extend the full distance to r_e ; a radial dimension of 15,000 ft will be sufficient to illustrate the primary features of the flow field. Transfer the interpolated stream functions from Fig. 15 to the arithmetic scale plot, indicating clearly the location of the point at which each stream function value applies. When all of these points have been transferred, construct the nine streamlines corresponding to stream function values of 0.1, 0.2, 0.3, 0.4, 0.5, 0.6, 0.7, 0.8 and 0.9, by contouring these values on the new plot. Next transfer a sufficient amount of head data from fig. 16 to the arithmetic scale flownet to allow the construction of lines of equal head, corresponding to 80, 85, 90, and 95 feet of head respectively. Keep in mind that in contrast to the stream function values, the head values actually apply at the node locations themselves.

The stream surfaces are not generally expected to be orthogonal (at right angles) to the surfaces of equal head because of the vertically exaggerated scale of the plot, and because the aquifer is anisotropic. However, where the flow occurs along one of the major axes of hydraulic conductivity, r or z, the condition of orthogonality applies.

When the head values have been contoured, we have completed our flow net in the r-z plane for the equilibrium condition of the radial flow system. Although both scales are arithmetic, there is still a considerable distortion because of the vertical exaggeration. Still, the figure tells us a number of important things about the system.

Flow-Net Interpretation

The streamlines and the lines of equal head on our flownet actually represent the intersection of three-dimensional stream surfaces or surfaces of equal head with the vertical r-z plane. The surfaces of equal head for 85 and 80 feet close completely around the screen; while no surfaces for lower values of head were constructed, these would obviously do the same thing. The surfaces for 90 and 95 feet close above the screen, but terminate against the bottom of the aquifer rather than closing below the well. Within the aquifer itself, significant differences (greater than 0.1 ft.) in head along the vertical persist to a radial distance of about four thousand feet from the well.

More than three quarters of the head loss in the system occurs within a radial distance of 250 feet from the well. Inside this radius, most of the flow occurs within the depth interval of the screen, in a pattern which is essentially horizontal. Most vertical movement is found at greater radial distances, where vertical hydraulic conductances are higher.

In the semiconfining unit, the stream surfaces are nearly vertical, while the surfaces of equal head would appear essentially horizontal except for the distortion of the vertical scale of the figure. Both the stream

surfaces and the surfaces of equal head are refracted at the contact between the semiconfining unit and the aquifer. Within the aquifer, the stream surfaces gradually reorient toward the horizontal pattern which prevails around the well screen, while the surfaces of equal head reorient into a pattern of closure around the screen. Because the aquifer itself is anisotropic (K_L/K_Z = 100) and the scale of the cross-section is exaggerated, the stream surfaces are in general not orthogonal to the surfaces of equal head within the aquifer. However, close to the well and within the screened interval, where the flow in predominantly parallel to the r axis, the condition of orthogonality prevails. Immediately above and below the screened interval, at short radial distances from the well, flow is nearly vertical and head gradients in the vertical are very steep.

Because the flow is largely horizontal and radial close to the well, the pattern here actually resembles that of the problem with which we started--radial flow toward a well in the center of an island. Thus, the Thiem equation (equation 5), could be used in an approximate sense to describe the system in this region; and the logarithmic "drawdown cone" around the well, predicted by the Thiem equation, characterizes this part of the system. This is true in virtually all discharging well problems--i.e., there is always a region around the well in which the dominant process is simply horizontal-radial flow, and in which head losses vary with the log of radial distance, so that gradients become very steep at small values of r.

Estimation of Lateral Hydraulic Conductivity from Pumpage Response Data

In this section, the symbol K and the term hydraulic conductivity refer to the lateral hydraulic conductivity of the aquifer.

Specific-capacity analysis--Some methods of estimating hydraulic conductivity from specific capacity take advantage of the "Thiem condition" in the area close to the well. In the problem for which equation (5) was formulated--radial flow to a well at the center of an island--we could assume that the head in the well prior to pumping was the same as the head at r_e during pumping-i.e., that the original or undisturbed head in the aquifer was equal to that in the open water surrounding the island, h_e. The head in the well during pumping, h_w, can be calculated by setting $r=r_w$ in equation (5), i.e.

$$h_w = h_e - \frac{Q_w}{2\pi Kb}(\ln r_e) + \frac{Q_w}{2\pi Kb}(\ln r_w) \qquad (20)$$

The drawdown in the well due to the pumping, s_w, is simply h_e-h_w. Solving (20) for this term gives

$$s_w = h_e - h_w = \frac{Q_w}{2\pi Kb}(\ln r_e - \ln r_w) = \frac{Q_w}{2\pi Kb} \ln (r_e/r_w) \qquad (21)$$

Then solving (21) for the hydraulic conductivity, K, gives

$$K = \frac{Q_w}{2\pi b s_w} \ln (r_e/r_w) \qquad (22)$$

Now suppose we wish to apply equation 22 in a more realistic problem of flow to a well, such as the one in our flownet; to do this, we must make the assumption that essentially all of the head loss, or drawdown, occurs close to the well, within some "radius of influence"--say 500 feet--and that within this radius, the flow occurs in a horizontal radial pattern, and is confined to the depth interval of the screen. Thus in place of the thickness of aquifer, b, of equation (22), we would use the screen length; and in place of the radius of the island, we would use the arbitrarily chosen radius of influence. In the problem illustrated in our flow net, we can make the assumption that prior to pumping the head in the well was equal to that along the constant head surface at the top of the semiconfining bed--i.e., 100 feet above datum. From figure 16, the head at the screen during pumping is approximately 35.5 feet; thus neglecting entrance losses the drawdown in the well is approximately 64.5 feet. As part 11 of the radial-flow problem, use this drawdown, a screen length of 40 feet, and a "radius of influence" of 500 feet to calculate the hydraulic conductivity of the aquifer material using equation 22. Repeat this calculation using a radius of influence of 100 feet and 1000 feet. Compare your answers to the value of hydraulic conductivity given for our problem, 100 gpd/ft^2. Note that small values of r_e yield small values of K; large values of r_e yield large values of K. Discuss the reasons for this relationship.

Distance-Drawdown Analysis--If equation (5) is differentiated with respect to ln r we obtain

$$\frac{dh}{d(\ln r)} = \frac{Q_w}{2\pi Kb}, \qquad (23)$$

since the terms h_e and $\frac{Q_w}{2\pi Kb} \ln r_e$ are both constants. This can be expressed in terms of common (base 10) logarithms simply by multiply by the constant 2.3. So, equation (23) becomes,

$$\frac{dh}{d(\log_{10} r)} = \frac{2.3Q_w}{2\pi Kb} \qquad (24)$$

or in terms of aquifer transmissivity

$$\frac{dh}{d(\log_{10} r)} = \frac{2.3Q_w}{2\pi T} \qquad (25)$$

The familiar distance-drawdown method of determining aquifer transmissivity from observation well data is based on equations 24-25. These equations can be derived from various nonequilibrium analyses as well as from equation (5), subject to the conditions that we are considering relatively small values of r, where flow is essentially horizontal, and that sufficient time has elapsed so that storage effects near the well are negligible; the distance-drawdown method is often applied in nonequilibrium analyses where these conditions are satisfied. Equation (25) tells us that if head is plotted against the log of r (or against r on semilog paper, with radial distance on the log axis) the plot should be a straight line with slope $(2.3Q_w/2\pi T)$. Thus determination of T should be possible simply by making such a plot from observation well data, measuring the slope and solving for T. Let's try to apply this method to the problem represented in our flow net. As part 12 of the radial-flow problem, use the head data in figure 16 to construct plots of head vs. distance on semilog paper for three different depths--100 feet, 140 feet and 180 feet below the top of the semiconfining bed. Carry each plot from the radius of influence, 32,768 feet, to the radius of the screen, 1 foot, plotting head on the arithmetic scale against radial distance on the log scale. Measure the slopes of these plots in the interior part of the system (r<500ft.), in feet of head change per log cycle of radial distance. (Note that the units of these slopes have the units of feet, since the log term is dimensionless.) Calculate three values of aquifer transmissivity by substituting the three measured values of slope, in turn, into equation (25) and solving for T. The actual transmissivity of our aquifer is 100 gpd/ft^2 x 100 ft = 10^4 gpd/ft. Discuss the reasons for any discrepancies among the three values you have calculated, and between these values and the actual transmissivity of the aquifer.

Now divide each calculated transmissivity by the aquifer thickness, 100 feet, to calculate a value of hydraulic conductivity for the aquifer material. Explain any discrepancies between the calculated values and the actual value, 100 gpd/ft^2. Finally, divide the transmissivity calculated from the head gradient at 140 ft by the thickness of the screened interval, 40 feet. Explain the discrepancies or agreement with the actual value which you observe in this calculated result. Also, explain why the graph of head for a depth of 140 feet flattens out further from the well.

Time of Travel Calculation

In flow-net analysis the expression

$$t = \frac{nL^2}{K\Delta h} \qquad (26)$$

is frequently used for the time of travel along a length L in a stream tube, where K is hydraulic conductivity, n is effective porosity, and Δh is the head loss over the distance L. This expression provides a convenient and accurate method of calculation so long as the head gradient $(\Delta h/L)$ is relatively constant over the interval L. In radial flow to a well, as we have seen, gradients tend to be relatively uniform at large radial distances, but change rapidly as we approach the well in the logarithmic "cone of depression"; moreover the problem we have postulated deals with an anisotropic system.

To develop a more convenient method of calculating time of travel under these circumstances, we recall that each stream tube (in a flow net representing steady-state conditions) may be thought of as a conduit, which always carries the same fluid discharge. Figure 17 shows a segment of a stream tube which is bounded by two surfaces taken at right angles to the flow. The bulk volume of the stream tube segment between the two surfaces is designated V, and the volume of moving fluid within the segment is therefore nV, where n is effective porosity. Let Δt designate the time required to replace completely this volume of water in the stream tube segment--that is, Δt is the time required for a volume of water nV to pass the upstream surface of the segment, and for an equal volume to cross the downstream surface. The flow rate through the stream tube is then equal to $\frac{nV}{\Delta t}$. The time interval (Δt) required to completely replace the water in the stream tube segment must equal the time of travel of fluid particles between the upstream and downstream surfaces of the segment. If we know the flow rate through the stream tube, q_s, we may equate it to the term $\frac{nV}{\Delta t}$, and solve for Δt to determine the time of travel through the stream tube segment, that is

$$\Delta t = \frac{nV}{q_s} \tag{27}$$

Thus to calculate time of travel through a stream tube segment we need simply divide the volume of water in the segment, nV, by the flow rate through the stream tube. For our flow net, the flow through each stream tube is given by $Q_w/10$, where Q_w is the well discharge. (Remember to convert gallons to ft^3 by multiplying gallons by 0.134) The volume of a given stream tube segment can be determined approximately by estimating the area of the segment, in the r-z plane, on our flownet (remembering to take into account any vertical scale distortion) and multiplying this area by $2\pi r$, where r is the mean radial distance from the well axis to the segment. This volume is then multiplied by effective porosity to yield the volume of moving water, and divided by $Q_w/10$ to yield the time of travel through the segment.

As part 13 of the radial-flow problem, use this method to estimate the time of travel through the 0.4 - 0.5 stream tube from the top of the aquifer (that is, from the bottom of the confining bed) to the screen. Divide the stream tube (within the aquifer) into five segments for purposes of this calculation. Take the innermost segment as the portion of the streamtube between the well screen and a radius of 500 feet, and the next segment between radii of 500 and 1000 feet. Make the other divisions at 2000 feet and 3000 feet. Assume the effective porosity to be 0.20.

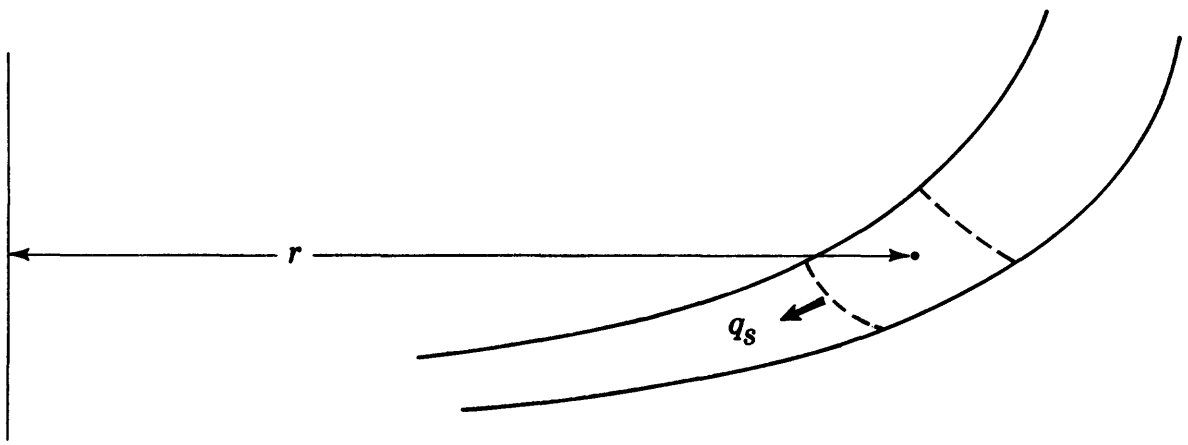

Figure 17 - Stream tube segment showing mean radius, r, from well axis

NOTE ON TRANSIENT RESPONSE

In the model design exercise, we divided the region around the well into cylindrical elements coaxial with the well, for purposes of specifying hydraulic conductance and storage capacity. When we attempt to visualize the transient response of, for example, a semiconfined aquifer to well discharge, it frequently is helpful to think of the region around the well as divided in this way into a succession of coaxial cylindrical shells. Withdrawal of water from the well may be thought of as establishing, initially, a hydraulic gradient between the well and the innermost shell; this causes flow from this innermost shell into the well. In general, this initial flow is supplied primarily by withdrawal from compressive storage close to the well, that is within the innermost shell; and this storage withdrawal is accompanied by a decrease in head with time. This head decrease establishes a gradient between the innermost shell and the second shell and creates inward flow between the two; this flow is supplied by storage withdrawal in the second shell and tends to reduce storage withdrawal in the innermost shell. This process continues with time, so that the effect of pumpage spreads progressively further out into the aquifer. As a result, the area of the aquifer supplying the largest share of storage withdrawal shifts steadily outward with time. Because we are considering a semiconfined aquifer, the effect of pumping spreads vertically as well as radially outward generating vertical flow, coupled with storage release in the confining beds. Ultimately the effect of pumping may reach the water table, where withdrawals can be maintained with much smaller drawdowns, or where reduction of natural outflow may supply a part of the pumpage. Again, these effects tend to migrate radially outward with time, so that the area of the water table that functions as the major source of water shifts outward as pumping continues. Ultimately a condition may be reached in which the reduction in natural outflow at the free surface balances the pumpage, and an equilibrium is achieved.

SUMMARY

This note has illustrated some of the basic characteristics of radial flow to a well. The particular example used in the simulation flow-net problem is certainly not representative of all radial flow systems; these systems obviously differ widely depending on the existing or postulated boundary and initial conditions, and the distribution of transmission and storage properties within the flow regime. Certain characteristics, however, are common to a wide variety of discharging well problems, and these are illustrated in the example.

For example, the steep decline in head approaching the well--that is, the logarithmic "cone of depression" around the screen or open interval--is present in all instances of flow to a well, because it is generated by the decreasing area of flow in the radial flow pattern. This implies that a large fraction of the head loss associated with well discharge must always occur near the well, within this logarithmic cone. Thus the material near a well exercises a strong influence on well performance, or specific capacity; and hydraulic conductivity estimates derived from specific capacity testing normally characterize the material near the screen.

The presence of the logarithmic cone of depression immediately around a discharging well is a function also of geometric controls on the processes of recharge, vertical flow and storage release. These processes all depend on horizontal (map) area. Near the well, the area available to support these processes is limited relative to that at greater radial distances. Thus, most of the accretion, storage release, or vertical flow convergence associated with a discharging well tends to occur at some distance from the well itself, where the available map area is greater. This in turn implies that there will generally be a zone around the well in which the flow is essentially horizontal, nearly equal to the well discharge, and restricted largely to the screened or open interval of the well. This zone represents the inner part of the cone of depression, and the straight-line portion of a semilog plot of drawdown vs. distance. The radial distance from the well to which this zone extends may vary greatly from one case to another, depending on the aquifer hydraulic properties, aquifer thickness, screen dimensions and boundary conditions; but generally there will always be some radius within which these conditions are approximated.

While the geometry of the well-aquifer system thus dictates a number of characteristics that are common to many radial flow problems, significant differences also exist from one situation to another. These may include differences in the boundary conditions of the problem, or differences in the distribution of hydraulic properties within the zone of influence of the well.

In some cases it has been possible to characterize a class or category of well-flow problems in terms of idealized boundary conditions and hydraulic property distribution, and to develop an analytical solution to the differential equation of radial flow for that category. For example, where the aquifer can be considered infinite in extent, perfectly confined and homogeneous; the well is fully penetrating and operates at constant discharge; and the pumpage is supplied entirely by withdrawal from compressive storage within the aquifer, the solution of Theis (1935) can be applied.

Where these conditions apply except that the well operates at a constant drawdown rather than constant discharge, the solution of Jacob and Lohman (1952) may be used. Where partial penetration of the well is a factor, the solutions of Kirkham (1959) or Hantush (1961) may be applicable. Where vertical leakage through confining beds is a factor, the solutions of Jacob (1946) or Hantush and Jacob (1955) may be applicable; and where storage release in the confining beds is significant the solution of Hantush (1960) may be used. The effect of vertical flow from a free surface, or water table is given in the solutions of Boulton (1954, 1963) and Neuman (1972).

The references given above represent only a few examples of the available analytical solutions for problems of radial flow to a well. They are included here to illustrate the fact that differences, as well as common elements, characterize problems of radial flow; and that where these differences can be expressed in terms of relatively simple boundary conditions and hydraulic parameter distributions, analytical solutions can sometimes be found. In applying solutions of this sort, it is important to examine carefully the degree to which the field situation conforms to the boundary conditions and distribution of hydraulic characteristics assumed in the solution. This conformity is never perfect, although frequently it is sufficient to permit useful approximation.

Finally, some of the principles underlying the simulation of radial flow have been presented in this note. In many situations the performance of a well, the interpretation of an aquifer test, or the evaluation of a ground water sampling event are addressed most effectively through simulation. Both finite difference and finite element methods have been used in radial flow simulation; and virtually any two-dimensional model program can be employed for this purpose, either through minor modification of the code or through appropriate specifications of input parameters.

APPENDIXES

A-I Derivation of Flow Equations--Axially Symmetric Flow, r-z Plane

Consider a ring shaped volume element of rectangular cross section, as shown in figure A-1. As in the preceding problem, we will use cylindrical coordinates and assume that flow occurs in both the r and z directions, but that axial symmetry exists, so that we need not consider the angular coordinate. We consider flow in the vertical direction to be positive if directed upward, and flow in the radial direction to be positive if directed outward. We assume that the medium exhibits simple two-dimensional anisotropy, with principal axes of hydraulic conductivity in the horizontal and vertical directions.

The volume element of figure A-1 extends from an inner radius r_1 to an outer radius r_2, and from a lower surface at z_3 to an upper surface at z_4; the radial width of the element is designated Δr, and its height is designated Δz. The inner cylindrical face of the element (at r_1) has an area $2\pi r_1 \Delta z$, while the outer cylindrical face has an area $2\pi r_2 \Delta z$. The radial flow into the element through the inner cylindrical surface is given by Darcy's law as

$$q_{r_1} = -K_L \cdot 2\pi r_1 \Delta z \left(\frac{\partial h}{\partial r}\right)_1 \qquad \text{(A-1)}$$

Where K_L is the lateral hydraulic conductivity and $\left(\frac{\partial h}{\partial r}\right)_1$ is the radial head gradient at r_1. The radial outflow from the element through the outer cylindrical face is similarly

$$q_{r_2} = -K_L \cdot 2\pi r_2 \Delta z \left(\frac{\partial h}{\partial r}\right)_2 \qquad \text{(A-2)}$$

The difference between radial inflow and radial outflow is therefore given by

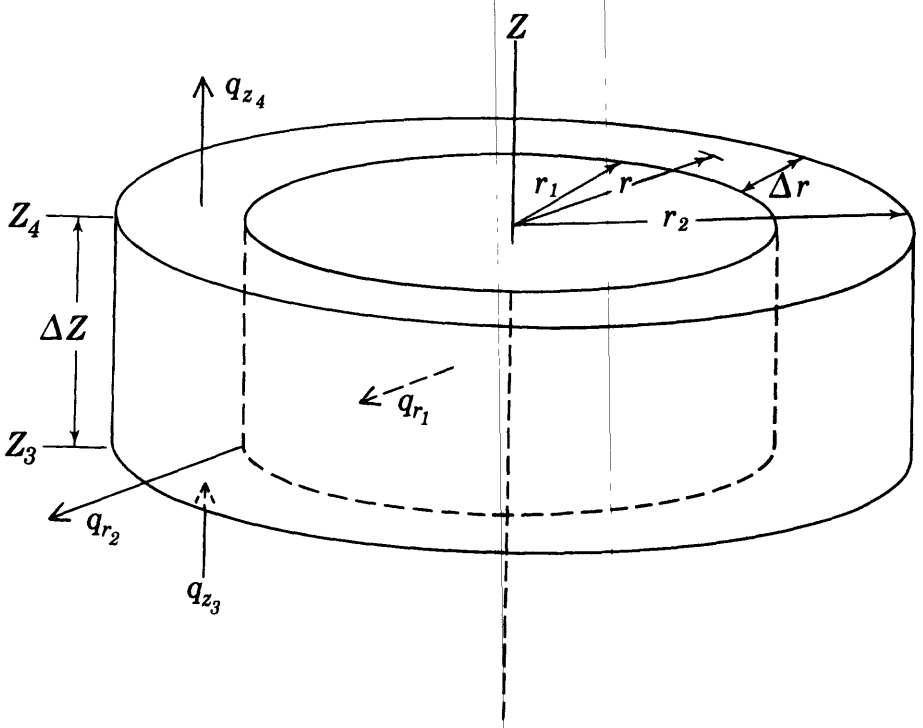

Figure A-1 - Cylindrical element volume illustrating axially symmetric flow

$$q_{r_1} - q_{r_2} = 2\pi K_L \Delta z \{ r_2 (\frac{\partial h}{\partial r})_2 - r_1 (\frac{\partial h}{\partial r})_1 \} \quad \text{(A-3)}$$

The term in brackets is given by the radial derivative of the function $r \frac{\partial h}{\partial r}$, multiplied by the radial width increment, Δr, i.e.

$$r_2 (\frac{\partial h}{\partial r})_2 - r_1 (\frac{\partial h}{\partial r})_1 \cong \frac{\partial}{\partial r} (r \frac{\partial h}{\partial r}) \Delta r \quad \text{(A-4)}$$

This is illustrated in figure A-2. The derivative on the right side of A-4 is in turn given (as the derivative of a product) by

$$\frac{\partial}{\partial r} (r \frac{\partial h}{\partial r}) = r \frac{\partial^2 h}{\partial r^2} + \frac{\partial h}{\partial r} \quad \text{(A-5)}$$

Thus we have for the difference between radial inflow and outflow

$$q_{r_1} - q_{r_2} = 2\pi K_L \Delta z \ (r \frac{\partial^2 h}{\partial r^2} + \frac{\partial h}{\partial r}) \Delta r \quad \text{(A-6)}$$

The vertical inflow to the element through the lower annular face is given by Darcy's law as

$$q_{z_3} = -K_z \pi (r_2^2 - r_1^2) (\frac{\partial h}{\partial z})_3 \quad \text{(A-7)}$$

Where K_z is the vertical hydraulic conductivity, $(\frac{\partial h}{\partial z})_3$ is the vertical gradient of head at the lower surface of the element (at z_3), and $\pi(r_2^2 - r_1^2)$ is the annular base area of the element.

Considering r to represent a mean radius of the element, we may substitute the terms $r - \frac{\Delta r}{2}$ for r_1 and $r + \frac{\Delta r}{2}$ for r_2 in (A-7). This gives

$$q_{z_3} = -K_z \cdot 2\pi r \Delta r (\frac{\partial h}{\partial z})_3 \quad \text{(A-8)}$$

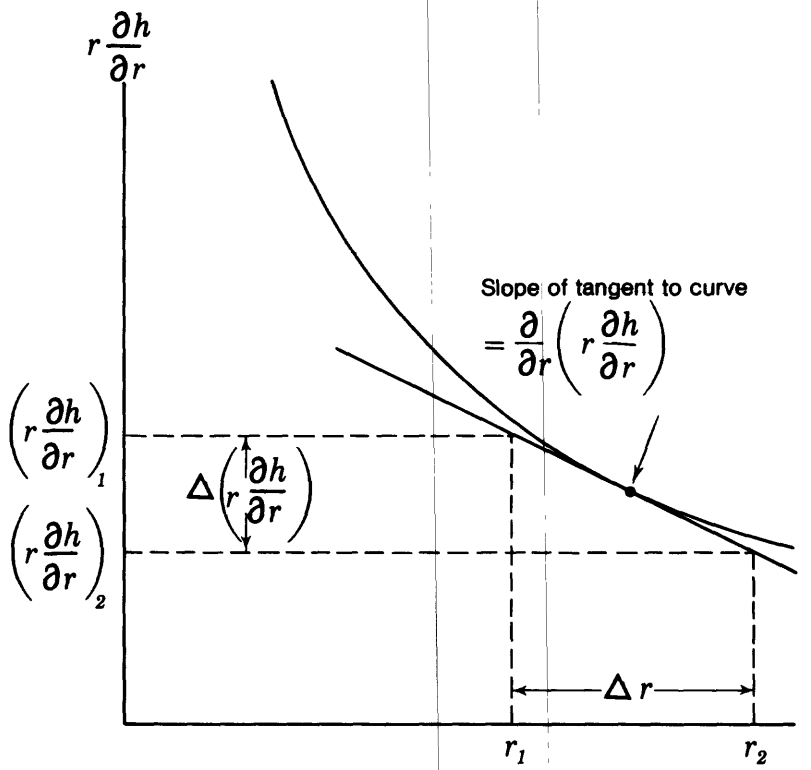

Figure A-2 - Plot of the function $(r\frac{\partial h}{\partial r})$ against r.

Similarly for the vertical outflow through the top of the element we have

$$q_{z_4} = -K_z \cdot 2\pi r \Delta r \left(\frac{\partial h}{\partial z}\right)_4 \tag{A-9}$$

The difference between vertical inflow and outflow is therefore

$$q_{z_3} - q_{z_4} = 2\pi K_z r \Delta r \left[\left(\frac{\partial h}{\partial z}\right)_4 - \left(\frac{\partial h}{\partial z}\right)_3\right] \tag{A-10}$$

or

$$q_{z_3} - q_{z_4} = 2\pi K_z r \Delta r \left(\frac{\partial^2 h}{\partial z^2}\right) \Delta z \tag{A-11}$$

The difference between total inflow and total outflow for the volume element is therefore

$$q_{r_1} - q_{r_2} + q_{z_3} - q_{z_4} = 2\pi \Delta r \Delta z \left\{K_L \left(r \frac{\partial^2 h}{\partial r^2} + \frac{\partial h}{\partial r}\right) + K_z r \frac{\partial^2 h}{\partial z^2}\right\} \tag{A-12}$$

or

$$q_{r_1} - q_{r_2} + q_{z_3} - q_{z_4} = 2\pi r \Delta r \Delta z \left\{K_L \left(\frac{\partial^2 h}{\partial r^2} + \frac{1}{r}\frac{\partial h}{\partial r}\right) + K_z \frac{\partial^2 h}{\partial z^2}\right\} \tag{A-13}$$

The rate of accumulation of water in storage in the element, assuming that it does not contain a free surface, is given by the product of specific storage, element volume, and time derivative of head, i.e.

$$\frac{dv}{dt} = S' \pi (r_2^2 - r_1^2) \Delta z \frac{\partial h}{\partial t} \tag{A-14}$$

where S' is specific storage; or again using $r - \frac{\Delta r}{2}$ for r_1 and $r + \frac{\Delta r}{2}$ for r_2,

$$\frac{dv}{dt} = S' 2\pi r \Delta r \Delta z \frac{\partial h}{\partial t} \tag{A-15}$$

Equating the rate of accumulation in (A-15) to the net difference between inflow and outflow from (A-13), and dividing by the term $2\pi r\Delta r\Delta z$, we have

$$K_L\left\{\frac{\partial^2 h}{\partial r^2} + \frac{1}{r}\frac{\partial h}{\partial r}\right\} + K_z\frac{\partial^2 h}{\partial z^2} = S'\frac{\partial h}{\partial t} \qquad \text{(A-16)}$$

Equation (A-16) is the partial differential equation for ground water flow in cylindrical coordinates, where there is no variation with the angular coordinate. It applies to all points in the interior of the system, and the term S' thus describes compressive or artesian storage processes.

A-II Water-Table Storage as a Boundary Condition

No free surface effects were present in the radial flow problems which we have considered. However, a question naturally arises as to how equation (A-16), which embodies compressive storage, could apply to a water table situation, where the dominant storage process is drainage or accumulation associated with change in water-table position. In addressing this question we must keep in mind that we are dealing with a cross section. When we simulate an unconfined aquifer, the free surface will be the upper boundary of our model; the process of water table storage occurs only along this boundary, and is thus properly treated as a boundary condition of equation (A-16). Compressive storage, as described by the term on the right of equation (A-16), is present in the interior of the system even in a water table aquifer, although its magnitude may be negligible in comparison to water table effects. In any case, when we are simulating a cross section in an unconfined situation, it's important to realize that water-table effects must be addressed as a boundary condition, and are not distributed through the interior of the flow system.

Boulton (1954) shows that when areal recharge to the water table is negligible, so that water table storage is the only process to be considered at the free surface, the equation

$$S_y \frac{\partial h}{\partial t} = K_L\left(\frac{\partial h}{\partial r}\right)^2 + K_z\left\{\left(\frac{\partial h}{\partial z}\right)^2 - \frac{\partial h}{\partial z}\right\} \qquad \text{(A-17)}$$

where S_y is specific yield, should be satisfied at all points on the water table, as a boundary condition of equation (A-16). While other boundary conditions on the free surface are certainly possible, a derivation of condition (A-17) is presented in the following paragraphs to demonstrate how the process of water-table storage can be accomodated even though a compressive storage expression, $S'\frac{\partial h}{\partial t}$, is used in (A-16).

The boundary condition expressed in equation (A-17) is obtained by considering the motion of an individual fluid particle in the free surface. An assumption is made that once a fluid particle becomes part of the free surface it remains within that surface (under this assumption, there can be no recharge crossing the water table from the unsaturated zone.) Pressure is assumed to be constant (i.e., atmospheric) on the water table; and since pressure in ground water systems is given by $\rho g(h-z)$, in which ρ is fluid density (assumed here to be constant) and g is the gravitational constant, it follows that (h-z) must be constant for particles in the free surface. Thus the derivation of (h-z) with respect to time, following the motion of a particle in the free surface, must be zero, i.e.

$$\frac{D(h-z)}{Dt} = \frac{\partial(h-z)}{\partial t} + \frac{v_r}{n}\frac{\partial(h-z)}{\partial r} + \frac{v_z}{n}\frac{\partial(h-z)}{\partial z} = 0 \qquad \text{(A-18)}$$

where $\frac{D(h-z)}{Dt}$ denotes differentiation following the motion of a particle in

the free surface, v_r is the component of the Darcy velocity in the radial direction, v_z its component in the vertical direction, and n is effective porosity; thus $\frac{v_r}{n}$ and $\frac{v_z}{n}$ are the components of the actual seepage velocity. $\frac{v_r}{n}$ therefore gives the rate of change of the radial coordinate of the particle with respect to time; multiplication of this term by $\frac{\partial(h-z)}{\partial r}$ gives that part of the rate of change of the term (h-z) with time which is due to movement of the particle along the r axis. Similarly $\frac{v_z}{n}\frac{\partial(h-z)}{\partial z}$ gives the rate of change of (h-z) with time due to vertical movement of the particle.

An assumption is then made that S_y, the specific yield, can be substituted for effective porosity in equation (A-18)--i.e., that the ratio of actual seepage area to gross area is equal to the specific yield, which is normally defined in terms of gravity drainage. Making this change, and substituting $-K_L\frac{\partial h}{\partial r}$ for v_r and $-K_z\frac{\partial h}{\partial z}$ for v_z, (A-18) becomes

$$\frac{D(h-z)}{Dt} = \left(\frac{\partial h}{\partial t} - \frac{\partial z}{\partial t}\right) - \frac{K_L}{S_y}\frac{\partial h}{\partial r}\left\{\frac{\partial h}{\partial r} - \frac{\partial z}{\partial r}\right\} - \frac{K_z}{S_y}\frac{\partial h}{\partial z}\left\{\frac{\partial h}{\partial z} - \frac{\partial z}{\partial z}\right\} = 0 \qquad \text{(A-19)}$$

In equation (A-19) the terms $\frac{\partial z}{\partial t}$ and $\frac{\partial z}{\partial r}$ are zero, while $\frac{\partial z}{\partial z} = 1$. Thus the equation becomes

$$\frac{\partial h}{\partial t} - \frac{K_L}{S_y}\left(\frac{\partial h}{\partial r}\right)^2 - \frac{K_z}{S_y}\left\{\left(\frac{\partial h}{\partial z}\right)^2 - \frac{\partial h}{\partial z}\right\} = 0 \qquad \text{(A-20)}$$

Rearrangement of (A-20) yields the boundary condition of (A-17). In many cases the terms $\left(\frac{\partial h}{\partial r}\right)^2$ and $\left(\frac{\partial h}{\partial z}\right)^2$ are negligibly small compared to $\frac{\partial h}{\partial z}$, so that (A-17) reduces to

$$S_y\frac{\partial h}{\partial t} = -K_z\frac{\partial h}{\partial z} \qquad \text{(A-21)}$$

This boundary condition (equation A-21) has been used by Neuman (1972) and Reilly (1984). Equation (A-21) describes a condition in which the downward

vertical flow per unit area in the free surface is equal to the release of water from storage per unit area by gravity drainage. Whereas (A-17) is a difficult condition to utilize either analytically or in simulation, (A-21) can be approximated readily in a model by adding a row at the top of the mesh in which only the processes of water table storage and vertical flow are simulated.

A-III Approximation of the Flow Equation in the Radial Flow Model

The differential equation (A-16),

$$K_L \left\{\frac{\partial^2 h}{\partial r^2} + \frac{1}{r}\frac{\partial h}{\partial r}\right\} + K_z \frac{\partial^2 h}{\partial z^2} = S'\frac{\partial h}{\partial t}$$

can be rewritten

$$\frac{K_L}{r^2}\frac{\partial^2 h}{\partial (\ln r)^2} + K_z \frac{\partial^2 h}{\partial z^2} = S'\frac{\partial h}{\partial t} \qquad \text{(A-22)}$$

(A-22) is obtained by noting that

$$\frac{\partial h}{\partial r} = \frac{\partial h}{\partial (\ln r)}\frac{\partial (\ln r)}{\partial r} = \frac{1}{r}\frac{\partial h}{\partial (\ln r)} \qquad \text{(A-23)}$$

and, differentiating (A-23) with respect to r,

$$\frac{\partial^2 h}{\partial r^2} = \frac{1}{r}\cdot\frac{\partial}{\partial r}\left(\frac{\partial h}{\partial (\ln r)}\right) + \frac{\partial h}{\partial (\ln r)}\frac{-1}{r^2} = \frac{1}{r^2}\frac{\partial^2 h}{\partial (\ln r)^2} - \frac{1}{r^2}\frac{\partial h}{\partial (\ln r)} \qquad \text{(A-24)}$$

Substituting (A-23) and (A-24) into (A-16) yields equation (A-22).

Referring to figure A-3, the finite difference approximation for $\frac{\partial^2 h}{\partial (\ln r)^2}$ at a node i,j in a finite difference mesh in which columns (index j) are spaced at uniform intervals of ln r, while rows (index i) are spaced at uniform intervals of z, is given by

$$\left(\frac{\partial^2 h}{\partial (\ln r)^2}\right)_{i,j} = \frac{h_{i,\,j-1} + h_{i,j+1} - 2h_{i,j}}{(\Delta \ln r)^2} \qquad \text{(A-25)}$$

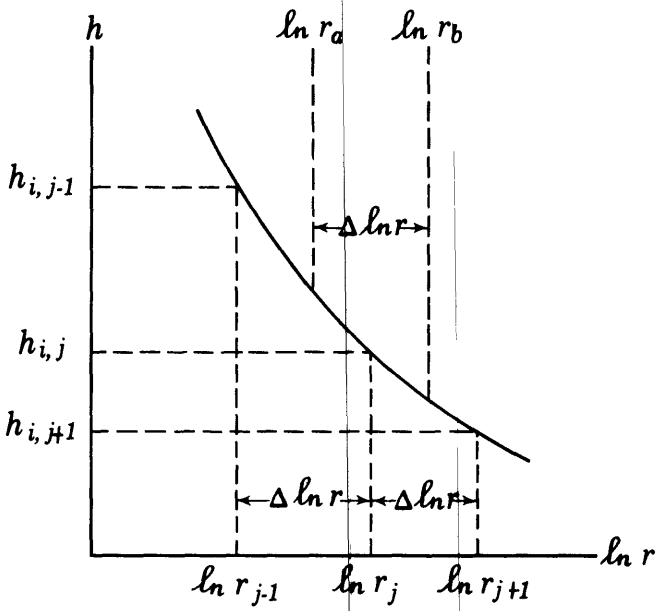

$$\frac{\partial h}{\partial (\ln r)_a} \approx \frac{h_{i,j} - h_{i,j-1}}{\Delta \ln r} \; ; \; \frac{\partial h}{\partial (\ln r)_b} \approx \frac{h_{i,j+1} - h_{i,j}}{\Delta \ln r}$$

$$\frac{\partial^2 h}{\partial (\ln r)^2_{i,j}} \approx \frac{\dfrac{h_{i,j+1} - h_{i,j}}{\Delta \ln r} - \dfrac{h_{i,j} - h_{i,j-1}}{\Delta \ln r}}{\Delta \ln r} \approx \frac{h_{i,j-1} + h_{i,j+1} - 2h_{i,j}}{(\Delta \ln r)^2}$$

Figure A-3.--Finite difference approximation of $\dfrac{\partial^2 h}{\partial (\ln r)^2}$ at node i, j.

Similarly the finite difference approximation for $\frac{\partial^2 h}{\partial z^2}$ at node i,j is

$$\left(\frac{\partial^2 h}{\partial z^2}\right)_{i,j} = \frac{h_{i-1,j} + h_{i+1,j} - 2h_{i,j}}{(\Delta z)^2} \tag{A-26}$$

The finite difference approximation for $\frac{\partial h}{\partial t}$ is given by

$$\frac{\partial h}{\partial t} = \frac{h_{i,j} - h^{*}_{i,j}}{\Delta t} \tag{A-27}$$

Where $h^{*}_{i,j}$ denotes the head at the central node, (i,j) at a time Δt prior to the time at which the heads of equations (A-25) and (A-26) are taken.

Substituting (A-25), (A-26) and (A-27) into equation (A-22), and setting $r=r_j$, where r_j is the radius associated with node i,j gives

$$\frac{K_L}{r_j^2} \frac{h_{i,j-1} + h_{i,j+1} - 2h_{i,j}}{\Delta(\ln r)^2} + K_z \frac{h_{i-1,j} + h_{i+1,j} - 2h_{i,j}}{(\Delta z)^2} = S' \frac{h_{i,j} - h^{*}_{i,j}}{\Delta t} \tag{A-28}$$

It may not be immediately apparent that the model utilized in the radial flow problem developed in this report addresses a system of equations of the form of (A-28). The following development is presented to demonstrate this.

Figure A-4 shows a sketch of a cylindrical volume element which contains the central node, i,j. In the finite difference formulations used in our model, inflow to node i,j in the outward radial direction is given by

$$Q_{i,j-1/2} = \frac{-2\pi K_L \Delta z}{\ln \alpha} (h_{i,j} - h_{i,j-1}) \tag{A-29}$$

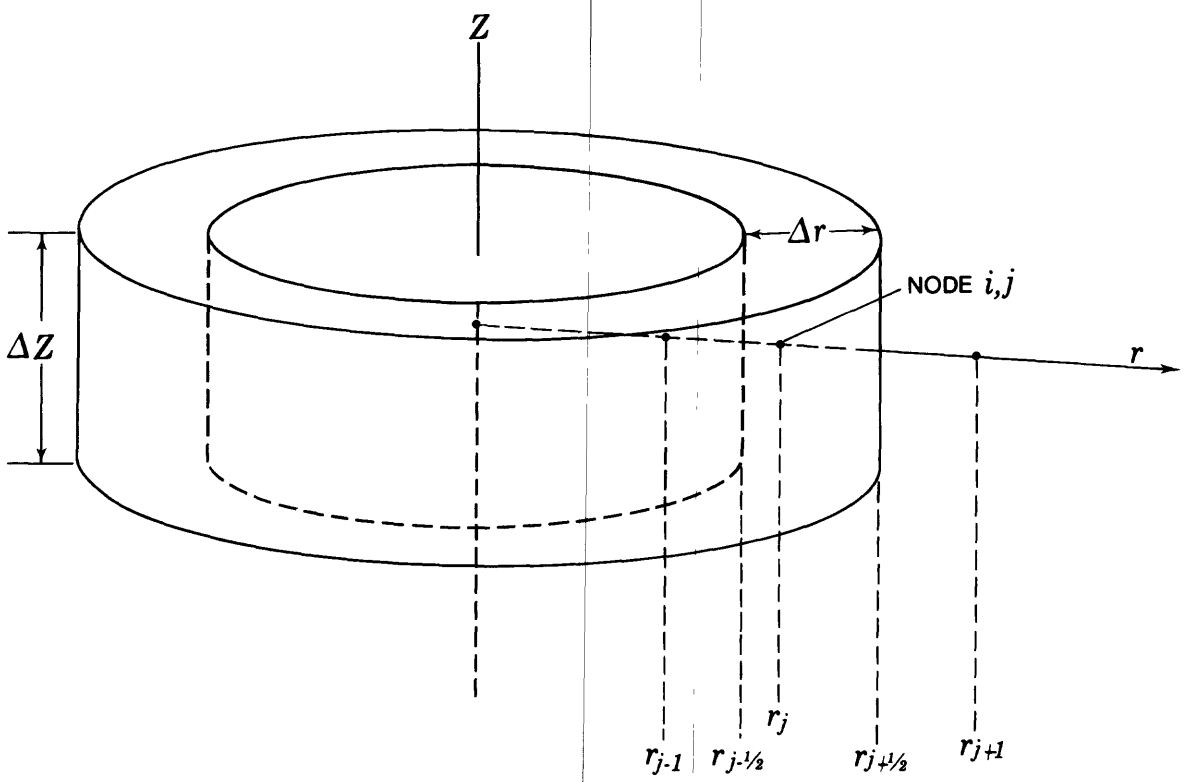

Figure A-4.--Cylindrical element volume containing the node i, j.

where α is the ratio $\frac{r_{j+1}}{r_j}$ which is assumed constant through the mesh and was taken as 2 in our simulation.

The term $\frac{h_{i,j} - h_{i,j-1}}{\ln \alpha}$ in equation (A-29) can be considered a finite difference approximation to the term $\frac{\partial h}{\partial (\ln r)}$ at the inner radius, $r_{j-1/2}$, of the volume element, since $\ln \alpha$ is equivalent to $(\ln r_j - \ln r_{j-1})$.

Radial outflow from node i, j to node i,j+1 is given by

$$Q_{i,j+1/2} = \frac{-2\pi K_L \Delta z}{\ln \alpha}(h_{i,j+1} - h_{i,j}) \qquad \text{(A-30)}$$

Vertical inflow in the upward direction from node i-1,j to node i,j is given by

$$Q_{i-1/2,j} = \frac{-K_z \pi (r^2_{j+1/2} - r^2_{j-1/2})}{\Delta z}(h_{i,j} - h_{i-1,j}) \qquad \text{(A-31)}$$

While vertical outflow from node i,j to node i+1,j is given by

$$Q_{i+1/2,j} = \frac{-K_z \pi (r^2_{j+1/2} - r^2_{j-1/2})}{\Delta z}(h_{i+1,j} - h_{i,j}) \qquad \text{(A-32)}$$

In equations (A-31) and (A-32), the term $\pi(r^2_{j+1/2} - r^2_{j-1/2})$ is given approximately by the expression

$$\pi(r^2_{j+1/2} - r^2_{j-1/2}) = 2\pi r_j \Delta r \qquad \text{(A-33)}$$

where

$$\Delta r = r_{j+1/2} - r_{j-1/2}$$

and the expression becomes exact if r_j falls at the arithmetic midpoint of $r_{j-1/2}$ and $r_{j+1/2}$. Substituting (A-33) into (A-31) gives

$$Q_{i-1/2,j} = \frac{-K_z \cdot 2\pi r_j \Delta r}{\Delta z}(h_{i,j} - h_{i-1,j}) \qquad \text{(A-34)}$$

Again using a finite difference approximation, the term Δr may be replaced by the term $r_j \Delta(\ln r)$, where $\Delta(\ln r)$ now represents the change in $\ln r$ from $r_{j-1/2}$ to $r_{j+1/2}$. This follows from the approximate relation

$$\frac{\Delta(\ln r)}{\Delta r} \doteq \frac{\partial(\ln r)}{\partial r} = \frac{1}{r} \tag{A-35}$$

This gives

$$Q_{i-1/2,j} = \frac{-K_z 2\pi r_j^2 \Delta(\ln r)}{\Delta z}(h_{i,j} - h_{i-1,j}) \tag{A-36}$$

In the same way we have for (A-32)

$$Q_{i+1/2,j} = \frac{-K_z 2\pi r_j^2 \Delta(\ln r)}{\Delta z}(h_{i+1,j} - h_{i,j}) \tag{A-37}$$

The rate of accumulation of water in storage at node i,j is approximated by

$$\frac{dv}{dt} = S' \cdot 2\pi r_j \Delta r \Delta z \frac{h_{i,j} - h^*_{i,j}}{\Delta t} \tag{A-38}$$

or again using $r_j \Delta(\ln r)$ for Δr,

$$\frac{dv}{dt} = S' 2\pi r_j^2 \Delta(\ln r) \Delta z \frac{h_{i,j} - h^*_{i,j}}{\Delta t} \tag{A-39}$$

Equating the difference between total inflow and total outflow to the rate of accumulation in storage gives

$$Q_{i,j-1/2} - Q_{i,j+1/2} + Q_{i-1/2,j} - Q_{i+1/2,j} =$$

$$\frac{2\pi K_L \Delta z}{\ln \alpha}(h_{i,j-1} + h_{i,j+1} - 2h_{i,j}) + \frac{2\pi K_z r_j^2 \Delta(\ln r)}{\Delta z}(h_{i-1,j} + h_{i+1,j} - 2h_{i,j})$$

$$= S' 2\pi r_j^2 \Delta(\ln r) \Delta z \frac{h_{i,j} - h^*_{i,j}}{\Delta t} \tag{A-40}$$

or, dividing by $2\pi\Delta z r_j^2 \Delta(\ln r)$ we have

$$\frac{K_L}{r_j^2 \Delta(\ln r)(\ln \alpha)} (h_{i,j-1} + h_{i,j+1} - 2h_{i,j}) +$$

$$\frac{K_z}{(\Delta z)^2} (h_{i-1,j} + h_{i+1,j} - 2h_{i,j}) =$$

$$S' \frac{h_{i,j} - h^*_{i,j}}{\Delta t} \qquad \text{(A-41)}$$

The inner and outer radii of the annular volume element of figure A-4, $r_{j-1/2}$ and $r_{j+1/2}$, were chosen so as to be given by

$$r_{j-1/2} = r_j \sqrt{\frac{2}{\alpha^2+1}} \qquad \text{(A-42)}$$

$$r_{j+1/2} = \alpha r_j \sqrt{\frac{2}{\alpha^2+1}} \qquad \text{(A-43)}$$

Thus these radii have the same ratio as do successive node radii, that is

$$\frac{r_{j+1/2}}{r_{j-1/2}} = \alpha \qquad \text{(A-44)}$$

$$\text{and } \Delta(\ln r) = \ln(r_{j+1/2}) - \ln(r_{j-1/2}) = \ln \alpha \qquad \text{(A-45)}$$

Therefore, substituting $\ln \alpha$ for $\Delta(\ln r)$ in (A-41) we have

$$\frac{K_L}{r_j^2 (\ln \alpha)^2}(h_{i,j-i} + h_{i,j+1} - 2h_{i,j})$$

$$+ \frac{K_z}{(\Delta z)^2} (h_{i-1,j} + h_{i+1,j} - 2h_{i,j})$$

$$= S' \frac{h_{i,j} - h^*_{i,j}}{\Delta t} \qquad \text{(A-46)}$$

Which is identical to equation (A-28). Thus the model used in our problem actually addresses a set of difference equations of the form of (A-28), and simulates the differential equations of (A-22) or (A-16).

Errors in the finite difference approximation are influenced by the choice of the outer and inner radii, $r_{j-1/2}$ and $r_{j+1/2}$, for the shell used in developing equation (A-29) through (A-46). An argument can be made that $r_{j-1/2}$ should be chosen so as to fall at the arithmetic midpoint of the interval between r_{j-1} and r_j, since in this case the relation of (A-33) would be satisfied exactly; an argument can also be made (Azis and Settari, 1979) for choosing $r_{j-1/2}$ to equal $\frac{r_j - r_{j-1}}{\ln(r_j/r_{j-1})}$. In any case, the errors associated with different choices of the intermediate radii will vary with the problem being simulated. The choice of intermediate radii which we utilized is intuitively appealing in that it provides an even distribution of storage and vertical conductance around each node; however, it does not guarantee that errors in the results will be minimum. One final point which should be noted is that any errors introduced by the choice of intermediate radii can be reduced by reducing α , i.e. the ratio $\frac{r_{j+1}}{r_j}$, in the design of the mesh. The closer α is to unity, the closer together all of the possible choices of intermediate radius will be.

A-IV - Answers to exercises and the radial-flow problem

Exercise 1:

Differentiate equation (4) with respect to r to show that it is a solution to the differential equation (equation 3).

Equation (4) is :

$$h = \frac{Q_w}{2\pi Kb} \ln r + C \qquad (4)$$

The terms $\frac{Q_w}{2\pi Kb}$ and C in equation 4 are constants. The derivative of ln r with respect to r is given by:

$$\frac{d(\ln r)}{dr} = \frac{1}{r}$$

Thus, when both sides of equation 4 are differentiated with respect to r we obtain:

$$\frac{dh}{dr} = \frac{Q_w}{2\pi Kb} \frac{1}{r}$$

This is equation 3, therefore equation 4 satisfies equation 3 and is a solution to the differential equation.

Exercise 2:

To obtain equation 7, use equation 5 to calculate h_1 and h_2 at r_1 and r_2 respectively. This gives:

$$h_1 = h_e - \frac{Q_w}{2\pi Kb} (\ln r_e) + \frac{Q_w}{2\pi Kb} (\ln r_1)$$

and

$$h_2 = h_e - \frac{Q_w}{2\pi Kb} (\ln r_e) + \frac{Q^w}{2\pi Kb} (\ln r_2)$$

where the equation for h_2 is the same as equation 6 in the text. If we

subtract h_1 from h_2 as follows:

$$h_2 - h_1 = h_e - \frac{Q_w}{2\pi Kb}(\ln r_e) + \frac{Q_w}{2\pi Kb}(\ln r_2) - h_e$$

$$+ \frac{Q_w}{2\pi Kb}(\ln r_e) - \frac{Q_w}{2\pi Kb}(\ln r_1)$$

the result is,

$$h_2 - h_1 = \frac{Q_w}{2\pi Kb}(\ln r_2 - \ln r_1)$$

which is equation 7.

Exercise 3: Calculation of radial conductances in table 1.

In all cases C_r = 150 gpd/ft. This is because in all cases $r_2/r_1 = 2$, or $r_2 = 2r_1$ To for calculate radial conductances, use equation 10 to get:

$$C_r = \frac{2\pi Kb\ (r_1 + r_2)/2}{r_2 - r_1}$$

substituting $2r_1$ for r_2 gives:

$$C_r = \frac{2\pi Kb\ (3r_1)/2}{r_1}$$

or

$$C_r = 3\pi Kb.$$

The final expression for the radial conductance is independent of r.

Exercise 4:

Verify that for any radius, r_a, the area between $r_a\sqrt{2/5}$ and r_a is equal to the area between r_a and $r_a\sqrt{8/5}$.

The area between $r_a\sqrt{2/5}$ and r_a is:

$$A_1 = \pi[r_a^2 - (r_a\sqrt{2/5})^2]$$

$$= \pi r_a^2 (1 - 2/5)$$

$$= \pi\ r_a^2 (3/5)$$

and the area between $r_a\sqrt{8/5}$ and r_a is:

$$A_2 = \pi[(r_a\sqrt{8/5})^2 - r_a^2]$$

$$= \pi r_a^2 (8/5 - 1)$$

$$= \pi r_a^2 (3/5) = A_1$$

Thus, $A_1 = A_2$.

RADIAL-FLOW PROBLEM:

Parts 1-3. See figure A-5 for the radii and depths

Part 4. They are cylindrical shells of rectangular cross section. From the top they look like donuts.

Part 5. The lateral conductances are calculated using, equation (13):

$$C_r = \frac{2\pi K_L \Delta z}{\ln 2} \qquad \text{and } \ln 2 = 0.693 .$$

Block	Lateral Conductance
A	$\frac{2\pi \times 25 \times 0.1}{0.693} = 22.7$
B	= A = 22.7
C	= A + G = 22.7 + 9067 = 9090
D	= C = 9090
E	$\frac{2\pi \times 20 \times 100}{0.693} = 18{,}130$
F	= E = 18,130
G*	$\frac{2\pi \times 10 \times 100}{0.693} = 9067$

*G may be as low as 9062 if you only use three significant digits for π.

Part 6. Note that $r_{j+1} = 2r_j$; see figure A-5 for answers.

Part 7. Note that $A_{j+1} = 4A_j$ (except for columns 1 and 16); see figure A-5 for answers.

Part 8. There are two equivalent methods of calculating vertical conductance:

a) Equation (17): $C_z = \frac{3.77 K_z r_a^2}{\Delta z}$

Note that $\frac{3.77 K_z}{\Delta z}$ is constant between any two rows. Between rows 4 and 5 it equals 0.1885 gpd/ft.

b) C_z = (Area calculated for question 7) x $K/\Delta z$

Column number	Vertical conductance	
	Method (a)	Method (b)
1	$1/2(0.1885 \times 1^2)$	$(1.886 \times 1)/20$
	$= 0.09425$	$= 0.00943$
2	(0.1885×2^2)	$(15.082 \times 1)/20$
	$= 0.754$	$= 0.754$
3	(0.1885×4^2)	$(60.33 \times 1)/20$
	$= 3.016$	$= 3.016$
4	(0.1885×8^2)	$(241.3 \times 1)/20$
	$= 12.064$	$= 12.065$
14	(0.1885×8192^2)	$(2.53 \times 10^8 \times 1)/20$
	$= 1.265 \times 10^7$	$= 1.265 \times 10^7$
15	$(0.1885 \times 16{,}384^2)$	$(1.01 \times 10^9 \times 1)/20$
	$= 5.060 \times 10^7$	$= 5.05 \times 10^7$
16	$1/2(0.1885 \times 32{,}768^2)$	$(2.02 \times 10^9 \times 1)/20$
	$= 1.012 \times 10^8$	$= 1.01 \times 10^8$

Discrepencies between methods (a) and (b) are due to round-off error.

Values from method (a) are shown on attached figure A-5.

Note that $C_{V_{j+1}} = 4\ C_{V_j}$ (except for columns 1 and 16, which use 1/2 cells in the calculation).

Part 9. There are two equivalent methods of calculating storage capacity:

a) Equation (18): $SC = \frac{6\pi S'\Delta z}{5} r_a^2$

Note that $\frac{6\pi S'\Delta z}{5}$ is constant

along any row. For row 7 it equals

$$\frac{6\pi(10^{-6})\ 20}{5} = 7.540 \times 10^{-5}$$

For row 8 it equals

$$\frac{6\pi(10^{-6})\ 10}{5} = 3.770 \times 10^{-5}$$

b) SC = (Area calculated for question 7) x S' x Δz

For row 7:

Column number	Storage capacity	
	Method (a)	Method (b)
1	$1/2(7.540 \times 10^{-5})\ 1^2$ $= 3.770 \times 10^{-5}$	$1.886 \times 10^{-6} \times 20$ $= 3.772 \times 10^{-5}$
2	$(7.540 \times 10^{-5})\ 2^2$ $= 3.016 \times 10^{-4}$	$15.082 \times 10^{-6} \times 20$ $= 3.016 \times 10^{-4}$
3	$(7.540 \times 10^{-5})\ 4^2$ $= 1.206 \times 10^{-3}$	$60.33 \times 10^{-6} \times 20$ $= 1.207 \times 10^{-3}$
4	$(7.540 \times 10^{-5})\ 8^2$ $= 4.826 \times 10^{-3}$	$241.3 \times 10^{-6} \times 20$ $= 4.826 \times 10^{-3}$
14	$(7.540 \times 10^{-5})\ 8192^2$ $= 5,060$	$(2.53 \times 10^{8}) \times 10^{-6} \times 20$ $= 5,060$
15	$(7.540 \times 10^{-5})\ 16,384^2$ $= 20,240$	$(1.01 \times 10^{9}) \times 10^{-6} \times 20$ $= 20,200$
16	$1/2(7.540 \times 10^{-5})\ 32,768^2$ $= 40,480$	$(2.02 \times 10^{9}) \times 10^{-6} \times 20$ $= 40,400$

Discrepencies between methods (a) and (b) are due to round-off error. Values from method (a) are shown on attached figure A-5.

Note that $SC_{j+1} = 4\ SC_j$ (except for columns 1 and 16)

For row 8, all values are 1/2 the value for the same colulmn in row 7 because Δz is now 10 instead of 20. See figure A-5.

The water released by a 1-foot drop in head in the block at row 7, column 16 is calculated by multiplying, SC, which has units of square feet, by 1 foot. So,

$$\Delta \text{ storage} = 40{,}480 \text{ ft}^2 \times 1 \text{ ft}$$
$$= 40{,}480 \text{ ft}^3$$
$$= 302{,}830 \text{ gallons}$$

10. See figure A-5.

The simulated discharge from each node representing the screen is Q/2, or 125,000 gallons per day.

Table A-1 gives the answers for table 2 on the calculation of stream functions.

Figure A-6 gives the answers for the stream function calculations shown on the model array.

The final flow net is shown in figure A-7. This is a quantitative flow net that shows the pattern of flow in the simlated system.

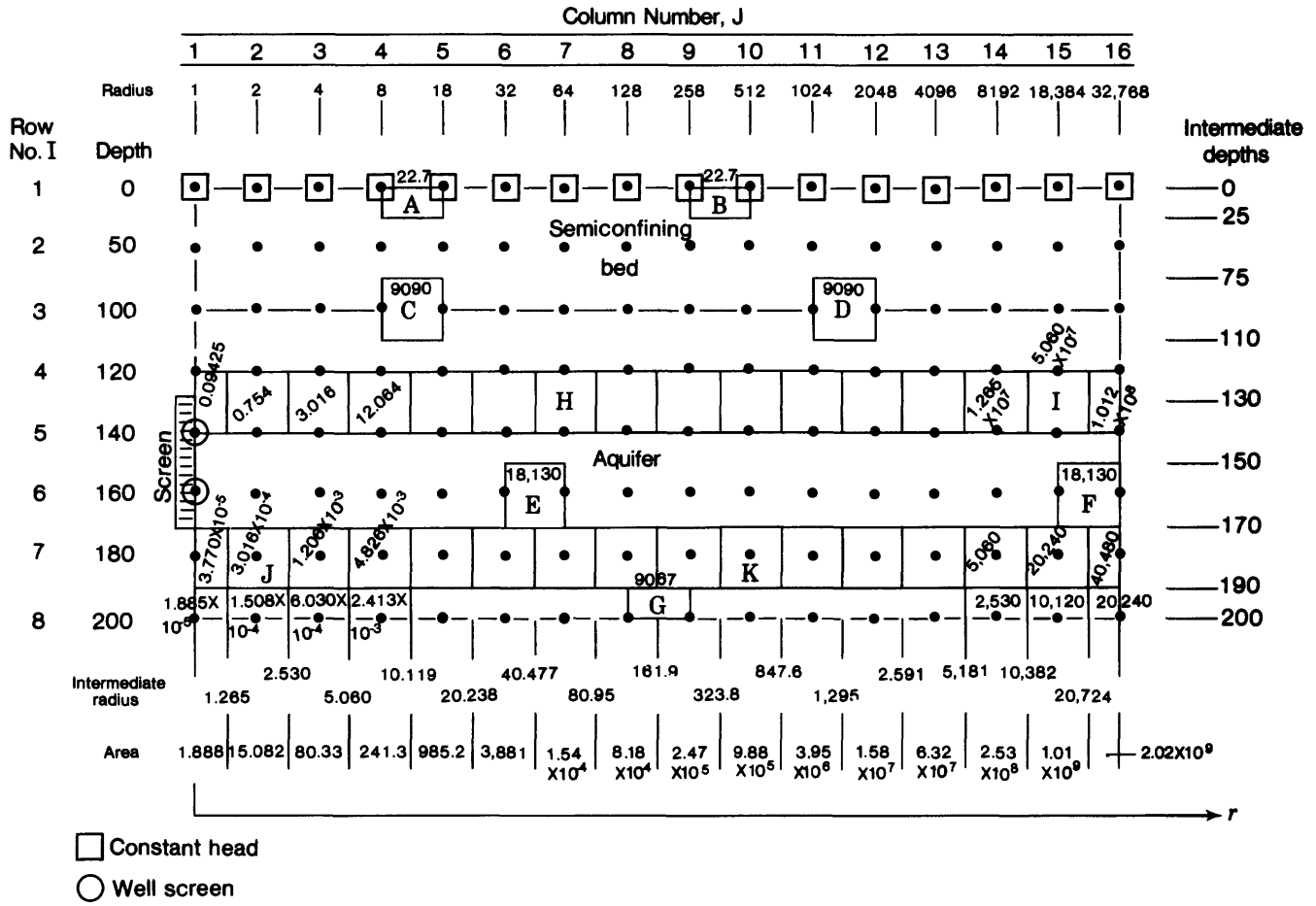

Figure A-5--Answers shown on model node array and volume elements used in calculating simulation coefficients.

Table - A-1
Table 2--Answers
Work Sheet for the Calculation of Stream Functions

Between columns	Row	Head drop Between Columns Δh (ft)	Lateral Hydraulic Conductance C_L (gpd/ft)	Flow through Conductance Block Q (gpd)	Cumulative Flow ΣQ (gpd)	Stream-Function Value $1 - \frac{\Sigma Q}{Q_T}$ (unitless)
15 & 16	8	0.02	9,067	181	181	0.9993
	7	0.02	18,130	363	544	0.9978
	6	0.02	18,130	363	907	0.9964
	5	0.02	18,130	363	1,270	0.9949
	4	0.02	18,130	363	1,633	0.9935
	3	0.02	9,090	182	1,815	0.9927
	2	0.01	45.4	0	1,815	0.9927
	1	0	22.7	0	1,815	0.9927
14 & 15	8	0.26	9,067	2,357	2,357	0.9906
	7	0.26	18,130	4,714	7,071	0.9717
	6	0.26	18,130	4,714	11,785	0.9529
	5	0.26	18,130	4,714	16,499	0.9340
	4	0.25	18,130	4,532	21,031	0.9159
	3	0.25	9,090	2,272	23,303	0.9068
	2	0.12	45.4	5	23,308	0.9068
	1	0	22.7	0	23,308	0.9068
13 & 14	8	1.02	9,067	9,248	9,248	0.9630
	7	1.02	18,130	18,490	27,738	0.8890
	6	1.01	18,130	18,310	46,048	0.8158
	5	1.00	18,130	18,130	64,178	0.7433
	4	0.99	18,130	17,950	82,128	0.6715
	3	0.97	9,090	8,817	90,945	0.6362
	2	0.49	45.4	22	90,967	0.6361
	1	0	22.7	0	90,967	0.6361
12 & 13	8	1.91	9,067	17,318	17,318	0.9307
	7	1.90	18,130	34,450	51,768	0.7929
	6	1.89	18,130	34,270	86,038	0.6558
	5	1.87	18,130	33,900	119,938	0.5202
	4	1.85	18,130	33,540	153,478	0.3861
	3	1.81	9,090	16,453	169,931	0.3203
	2	0.91	45.4	41	169,972	0.3201
	1	0	22.7	0	169,972	0.3201

Table A-1 (continued)
Table 2--Answers (continued)
Work Sheet for the Calculation of Stream Functions

Between columns	Row	Head Drop Between Columns Δh (ft)	Lateral Hydraulic Conductance C_L (gpd/ft)	Flow through Conductance Block Q (gpd)	Cumulative Flow ΣQ (gpd)	Stream-Function Value $1 - \frac{\Sigma Q}{Q_T}$ (unitless)
11 & 12	8	2.42	9,067	21,942	21,942	0.9122
	7	2.43	18,130	44,060	66,002	0.7360
	6	2.44	18,130	44,240	110,242	0.5590
	5	2.42	18,130	43,870	154,112	0.3836
	4	2.37	18,130	43,000	197,112	0.2116
	3	2.32	9,090	21,089	218,201	0.1272
	2	1.16	45.4	53	218,254	0.1270
	1	0	22.7	0	218,254	0.1270
10 & 11	8	2.43	9,067	22,033	22,033	0.9119
	7	2.57	18,130	46,594	68,627	0.7255
	6	2.86	18,130	51,852	120,579	0.5181
	5	2.85	18,130	51,670	172,149	0.3114
	4	2.52	18,130	45,690	217,839	0.1286
	3	2.34	9,090	21,271	239,110	0.0436
	2	1.16	45.4	53	239,163	0.0433
	1	0	22.7	0	239,163	0.0433
9 & 10	8	1.64	9,067	14,870	14,870	0.9405
	7	2.20	18,130	39,890	54,760	0.7810
	6	3.82	18,130	69,260	124,020	0.5039
	5	3.80	18,130	68,890	192,910	0.2284
	4	2.18	18,130	39,520	232,430	0.0703
	3	1.60	9,090	14,544	246,974	0.0121
	2	0.78	45.4	35	247,009	0.0120
	1	0	22.7	0	247,009	0.0120
7 & 8	8	0.21	9,067	1,904	1,904	0.9924
	7	0.65	18,130	11,780	13,684	0.9453
	6	6.14	18,130	111,320	125,004	0.5000
	5	6.13	18,130	111,140	236,108	0.0596
	4	0.65	18,130	11,780	247,888	0.0084
	3	0.21	9,090	1,909	249,797	0.0008
	2	0.09	45.4	4.1	249,801	0.0008
	1	0	22.7	0	249,801	0.0008

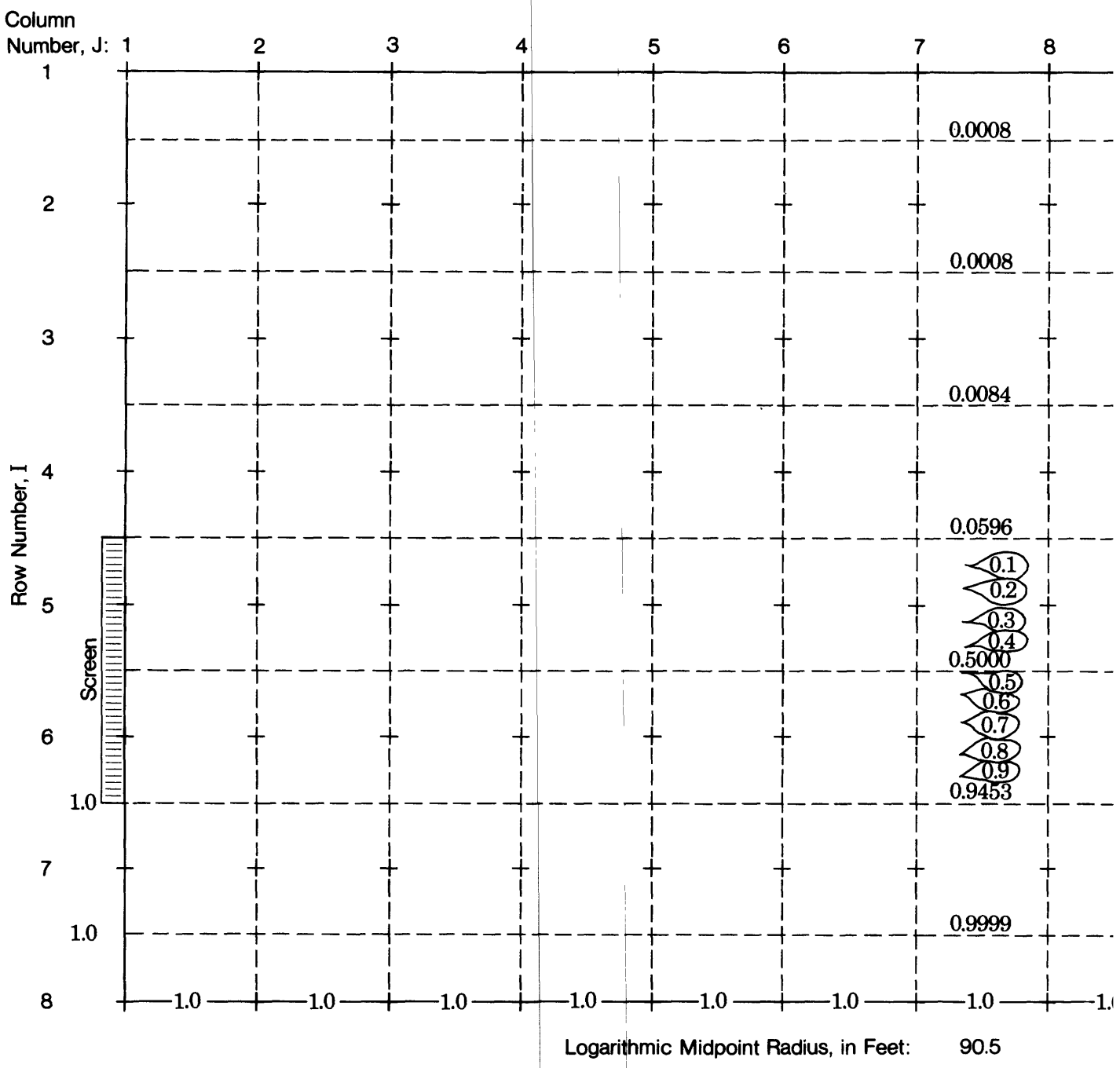

Figure A-6--Answers for stream function calculations shown on nodal array

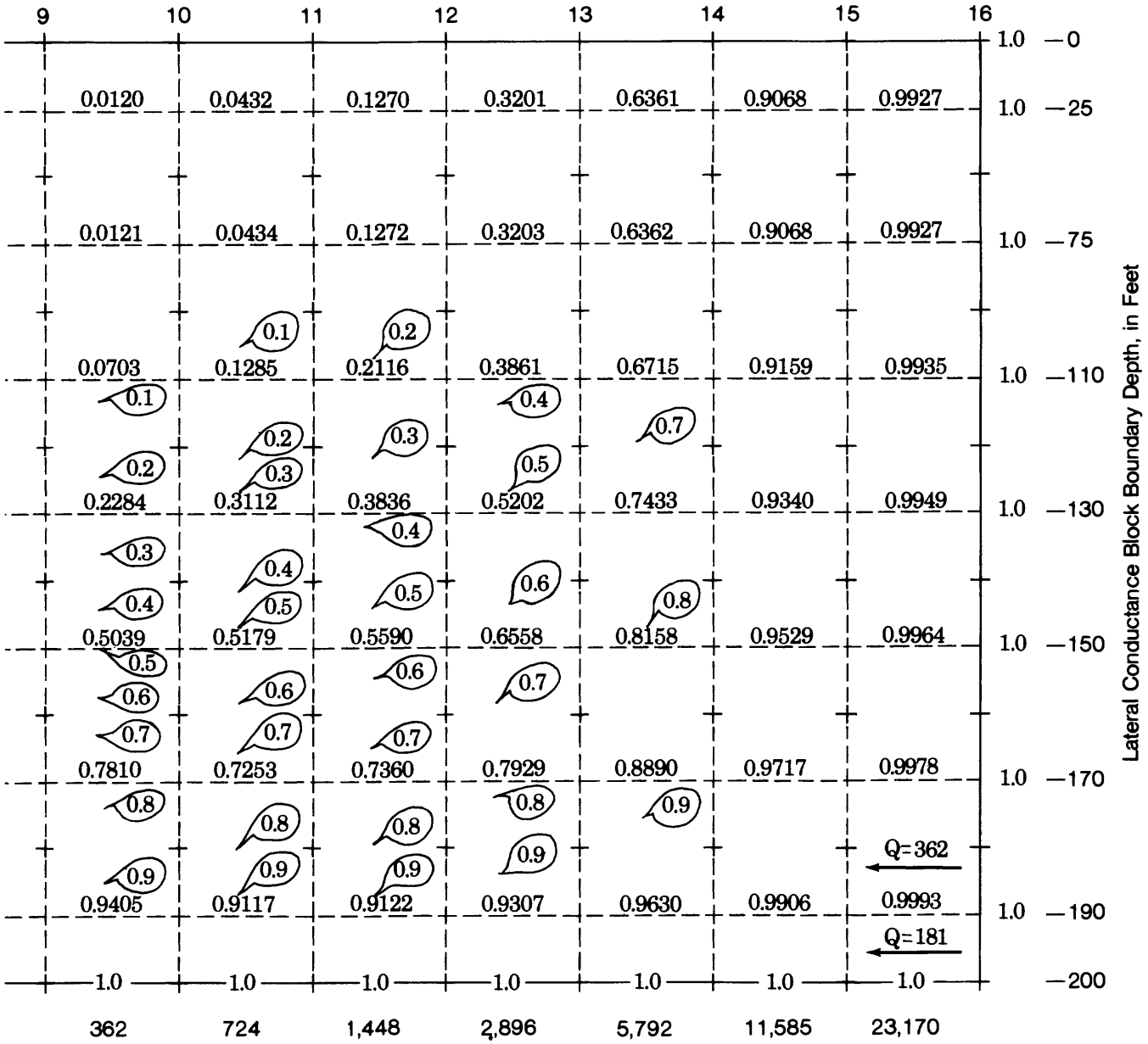

and lateral conductance block

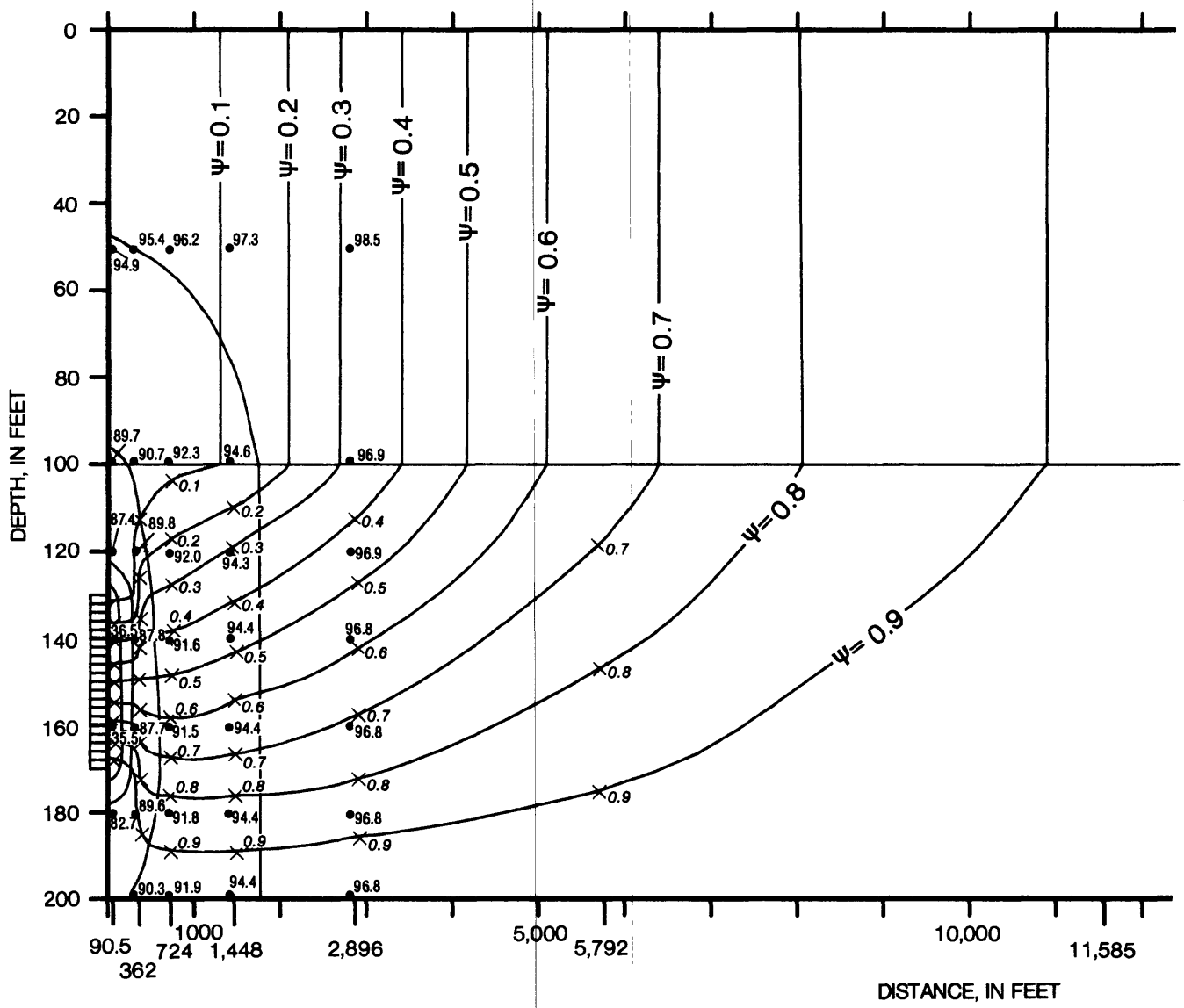

Figure A-7--Radial-flow net

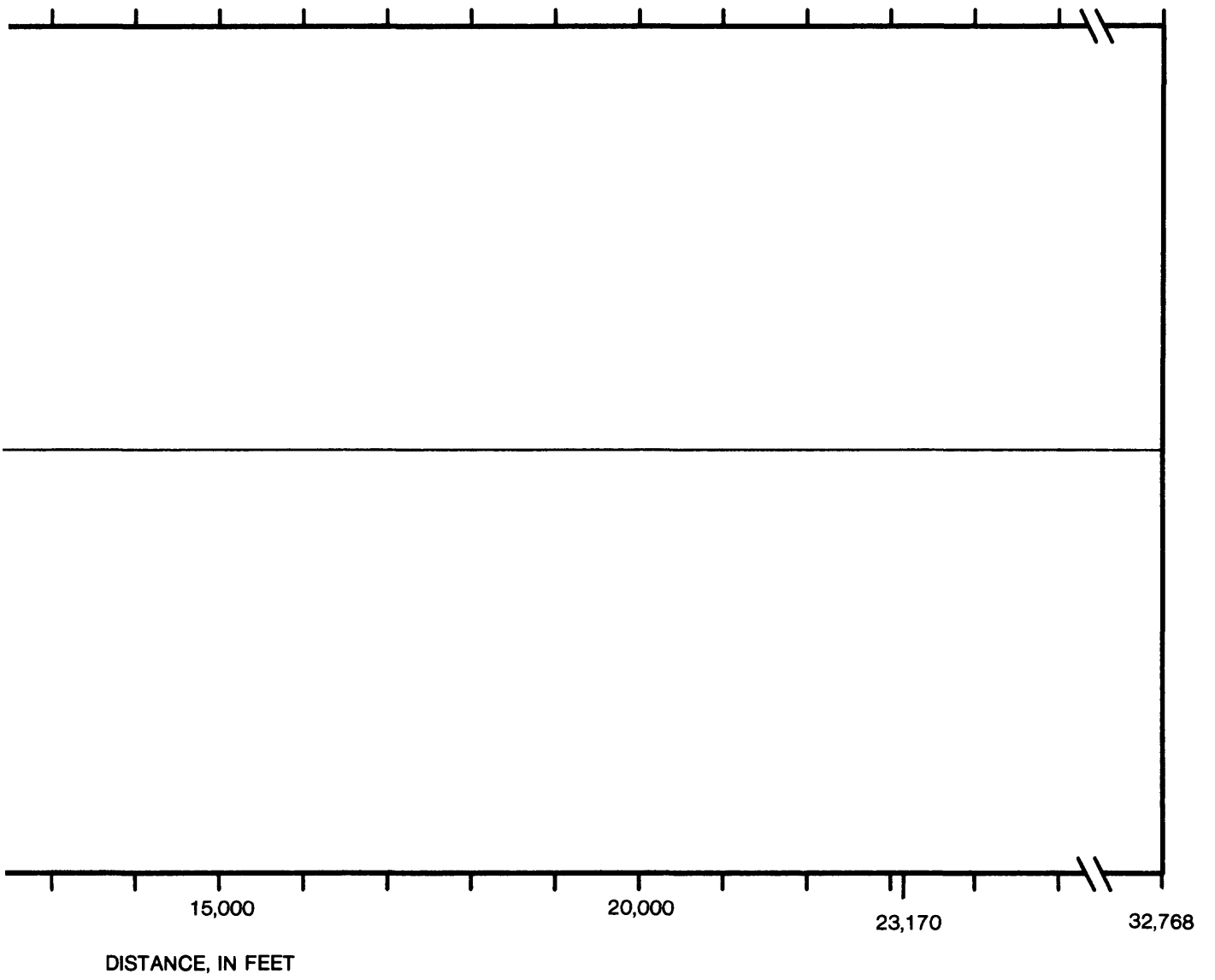
15,000
20,000
23,170
32,768
DISTANCE, IN FEET

Part 11. Calculate the lateral hydraulic conductivity of the aquifer using the drawdown at the well and equation (22), which is:

$$K = \frac{Q_w}{2\pi b s_w \ln(r_e/r_w)}$$

a) $r_e = 500$ ft

$$K = \frac{250{,}000 \text{ gpd}}{2\pi\ (40 \text{ ft})\ (64.5 \text{ ft})} \ln\frac{500}{(1)} = 95.8 \text{ gpd/ft}^2$$

b) $r_e = 100$ ft ; $K = 71.02$ gpd/ft^2

c) $r_e = 1{,}000$ ft ; $K = 106.53$ gpd/ft^2

Actually, $K = 100$ gpd/ft^2

Discussion:

Before discussing the relation between the computed K value and r_e it is useful to discuss the physical perspective that equation 22 implies. Equation 22 is based on the Thiem equation (equation 20 is one form of this equation). The Thiem equation is the mathematical solution to a purely one-dimensional radial problem with a constant head boundary at distance r_e. In a field case (or a more realistic problem such as our flownet), the flow field and boundary conditions are rarely that simple. In our flownet, the source of water is not a constant head source at r_e but rather is leakage from above over the entire problem domain. This causes vertical movement which is not consistent with the Thiem assumptions. The well is partially penetrating which also induced vertical movement. Thus, the field situation is much more complex than that represented by equation 22.

However, as stated in the problem, if we assume that essentially all of the head loss occurs close to the well and flow occurs in a purely radial form in the screen zone in this area close to the well, then use of the formula may have some relevance. We are left however, with two problems,

1) we do not know and can not measure an effective radius r_e that is appropriate and 2) we know that these assumptions are not completely correct. In many cases (perhaps even most cases), however, these assumption are reasonable. In these cases, estimating various effective radii give a good estimate of the general range of values for the hydraulic conductivity.

In our problem, the actual hydraulic conductivity was 100 gpd/ft^2. Estimates using three very different effective radii gave a range of 71 to 107 gpd/ft^2. This range gives a good indication of the actual hydraulic conductivity. Thus, this formula, based on a overly simplified system has value in quantifying field hydraulic conductivities.

In response to the relationship between hydraulic conductivity and effective radius, as can be observed in equation 22, the hydraulic conductivity (K) is proportional to the natural logarithm of the effective radius (ln r_e). Thus, as r_e increases so will K. Conceptually, the flow net shows that only a part of the well discharge, Q_w, occurs within the screened interval at any given radial distance from the well; and that only a part of the total head loss, s_w, (or $h_e - h_w$), occurs within any arbitrarily chosen "radius of influence", r_e. To the extent that the actual flow within the screened interval is less than Q_w we are using too large a flow value in our calculation, and our method will overestimate K; when we choose a large value of r_e, this tends to be the case, because the further we are from the well, the greater the percentage of the flow that falls outside the screened interval. To the extent that the head loss within our assumed value of r_e is less than the full head loss in the flow pattern, we are using too great a head loss value in our calculation and our method will underestimate K; when we choose a small value of r_e, this tends to be the case, as a greater proportion of the total head loss then occurs beyond r_e.

Part 12. Calculate T and K from distance - drawdown plots of heads at depths of 100 feet, 140 feet and 180 feet below the top of the confining layer using equation (25):

$$\frac{dh}{d\ (\log_{10} r)} = \frac{2.3\ Q_w}{2\pi T}$$

The distance drawdown plots for depths of 100 ft, 140 ft, and 180 ft are shown on figure A-8. Graphically estimated slopes over 1 log cycle are: a) 0.3 ft for the 100 ft deep curve, b) 21.5 ft for the 140 ft deep curve, and c) 1.1 ft for the 180 ft deep curve. The calculations for transmissivity and estimates of hydraulic conductivity using thicknesses of 100 and 40 ft are as follows:

a) 100 feet deep

$$\frac{0.3\ ft}{1} = \frac{2.3\ (250{,}000\ gpd)}{2\pi T} \quad ;\ T = 305{,}000\ gpd/ft$$

using b = 100 ft, $K = 3{,}050\ gpd/ft^2$

b) 140 feet deep

$$\frac{21.5\ ft}{1} = \frac{2.3\ (250{,}000\ gpd)}{2\pi T} \quad ;\ T = 4{,}260\ gpd/ft$$

using b = 100 ft, $K = 42.6\ gpd/ft^2$

using b = 40 ft, $K = 106\ gpd/ft^2$

c) 180 feet deep

$$\frac{1.1\ ft}{1} = \frac{2.3\ (250{,}000\ gpd)}{2\pi T} \quad ;\ T = 83{,}200\ gpd/ft$$

using b = 100 ft, $K = 832\ gpd/ft^2$

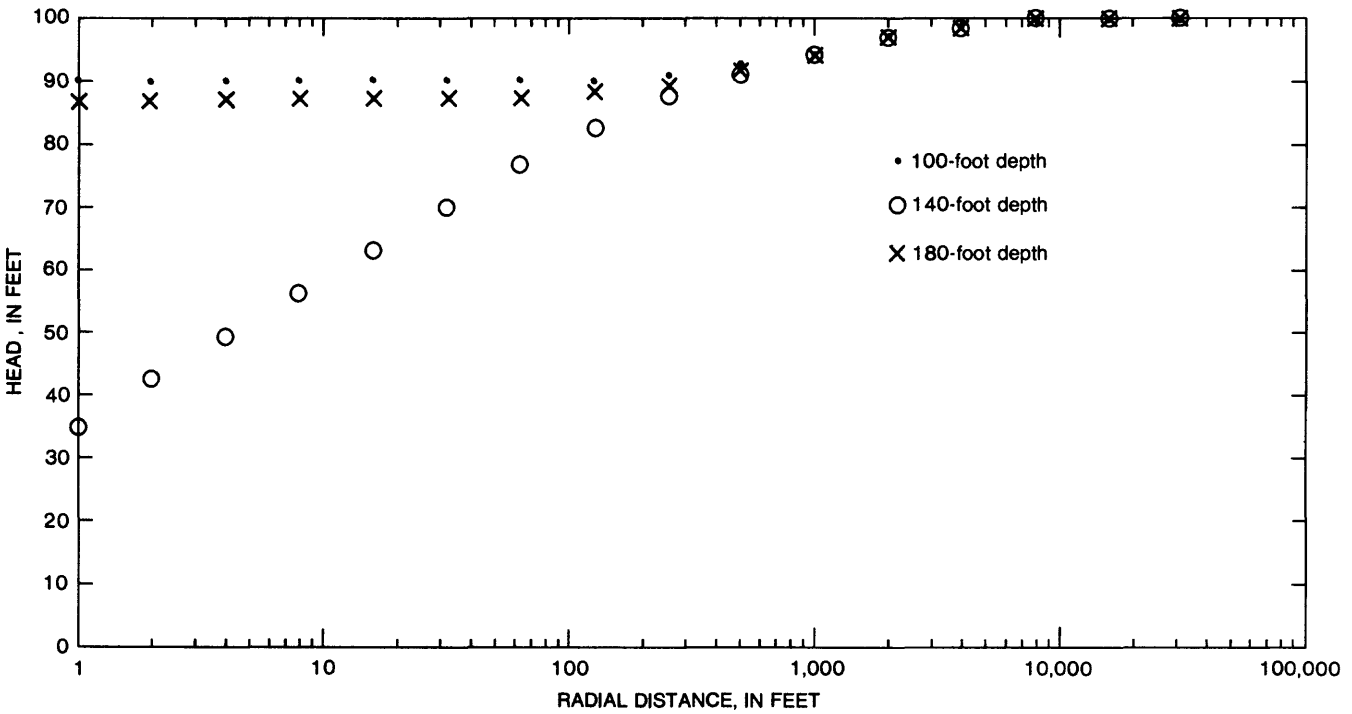

Figure A-8--Distance-drawdown graph

Discussion:

Discrepancies are due to the fact that the distance-drawdown approach does not take into account the vertical movement of water caused by leakage from the overlying confining unit, or the convergence of the flow pattern into the vertical interval tapped by the screen. Radial gradients above and below the screened interval--that is, at the 100 ft and 180 ft depths--are relatively low because the radial flow components at these depths are small. When these low gradients are associated with the full discharge of the well in equation (25), unreasonably high values of transmissivity are calculated. Division by the aquifer thickness yields correspondingly high values of hydraulic conductivity. At the 140 foot depth, the radial gradient reflects approximately the full discharge of the well, distributed through a forty-foot thickness of flow. When this gradient is used in equation (25) together with the full thickness of the aquifer, 100 feet, a transmissivity is calculated which is only about 40 percent of the actual aquifer transmissivity. If this transmissivity is divided by the full aquifer thickness, the resulting hydraulic conductivity is similarly about 40 percent of the actual value. However, if the calculated transmissivity is recognized as referring primarily to the screened interval, and is divided just by the thickness of that interval, the resulting hydraulic conductivity is relatively close to the true value. The six percent discrepancy arises because the actual thickness of the flow regime, over most of the interval in which the semilog slope is measured, is slightly greater than the screened interval.

The semilog plot of heads at the 140 foot depth flattens out with increasing distance from the well. In equation (24), the flow rate is taken as Q_w, the discharge from the well, and the vertical thickness of

the flow is taken as b, the aquifer thickness. Because these terms are both constants, we are led to the conclusion that the slop of the semilog plot, $\frac{dh}{d(\log_{10} r)}$, should be constant--that is it should not vary with r, nor in fact with z. Our flownet, however, as well as the calculations we have just done, show that these assumptions do not fit our problem very well. A more general expression for the slope of the semilog plot would be:

$$\frac{dh}{d \log_{10} r}(r,z_1) = \frac{2.3\ Q(r,z_1)}{2\pi K \Delta z}$$

where $\frac{dh}{d \log_{10} r}(r,z_1)$ represents the slope of a semilog plot of head vs. radial distance, in which the heads are all measured along a line of fixed elevation, z_1; and $Q(r,z_1)$ represents the discharge flowing radially toward the well at the elevation z_1, or actually through a small increment of height, Δz, which is centered on z_1. Our flownet shows us that if the elevation z_1, is within the screened interval--for example, the 140 foot depth--the flow $Q(r,z_1)$ must increase as we approach the well, for two reasons: first, the total flow in the system increases as we approach the well due to vertical accretion through the confining bed; and second, the flow must converge vertically into the screened interval as we approach the well. Thus, since $Q(r,z_1)$ increases with decreasing r, the slope of the semilog plot must do the same. At radial distances which are close to the well, both processes -- vertical accretion and flow convergence -- are essentially complete; the total flow is distributed more or less uniformly through a thickness equal to the screened interval. At these distances, therefore, the slope of the semilog plot at the 140

foot depth appears to be constant; and equation (24) gives a reasonable description of that slope so long as b is taken as the screened interval rather than the aquifer thickness. With increasing distance from the well, as $Q(r,z_1)$ decreases, the slope must decrease.

Part 13. Calculate the time of travel through the 0.4 to 0.5 stream tube using equation (27):

$$\Delta t = \frac{nV}{q_s},$$

where: $V = A\ 2\pi r_m$

For these calculations, the area (A) is obtained by graphically estimating the area between the .4 stream tube and the .5 stream tube in the r-z plane as shown on figure A-9. The calculations for each segment are:

Segment 1:

$$A = 2{,}700\ ft^2, \quad r_m = 250\ ft, \quad V = 4.24 \times 10^6\ ft^3$$

$$\Delta t = \frac{0.2\ V}{3{,}350\ ft^3/d} = 253\ days$$

Segment 2:

$$A = 5{,}300\ ft^2, \quad r_m = 750\ ft, \quad V = 2.49 \times 10^7\ ft^3$$

$$\Delta t = \frac{0.2\ V}{3{,}350\ ft^3/d} = 1{,}490\ days$$

Segment 3:

$$A = 11{,}000\ ft^2, \quad r_m = 1{,}500\ ft, \quad V = 1.04 \times 10^8\ ft^3$$

$$\Delta t = \frac{0.2\ V}{3{,}350\ ft^3/d} = 6{,}210\ days$$

Segment 4:

$$A = 12{,}600\ ft^2, \quad r_m = 2{,}500\ ft, \quad V = 1.98 \times 10^8\ ft^3$$

$$\Delta t = \frac{0.2\ V}{3{,}350\ ft^3/d} = 11{,}800\ days$$

Segment 5:

$$A = 14{,}400\ ft^2, \quad r_m = 3{,}500, \quad V = 3.17 \times 10^8\ ft^3$$

$$\Delta t = \frac{0.2\ V}{3{,}350\ ft^3/d} = 18{,}900\ days$$

Time of travel through the entire stream tube equals the sum of all segments which is 38,700 days, or 106 years.

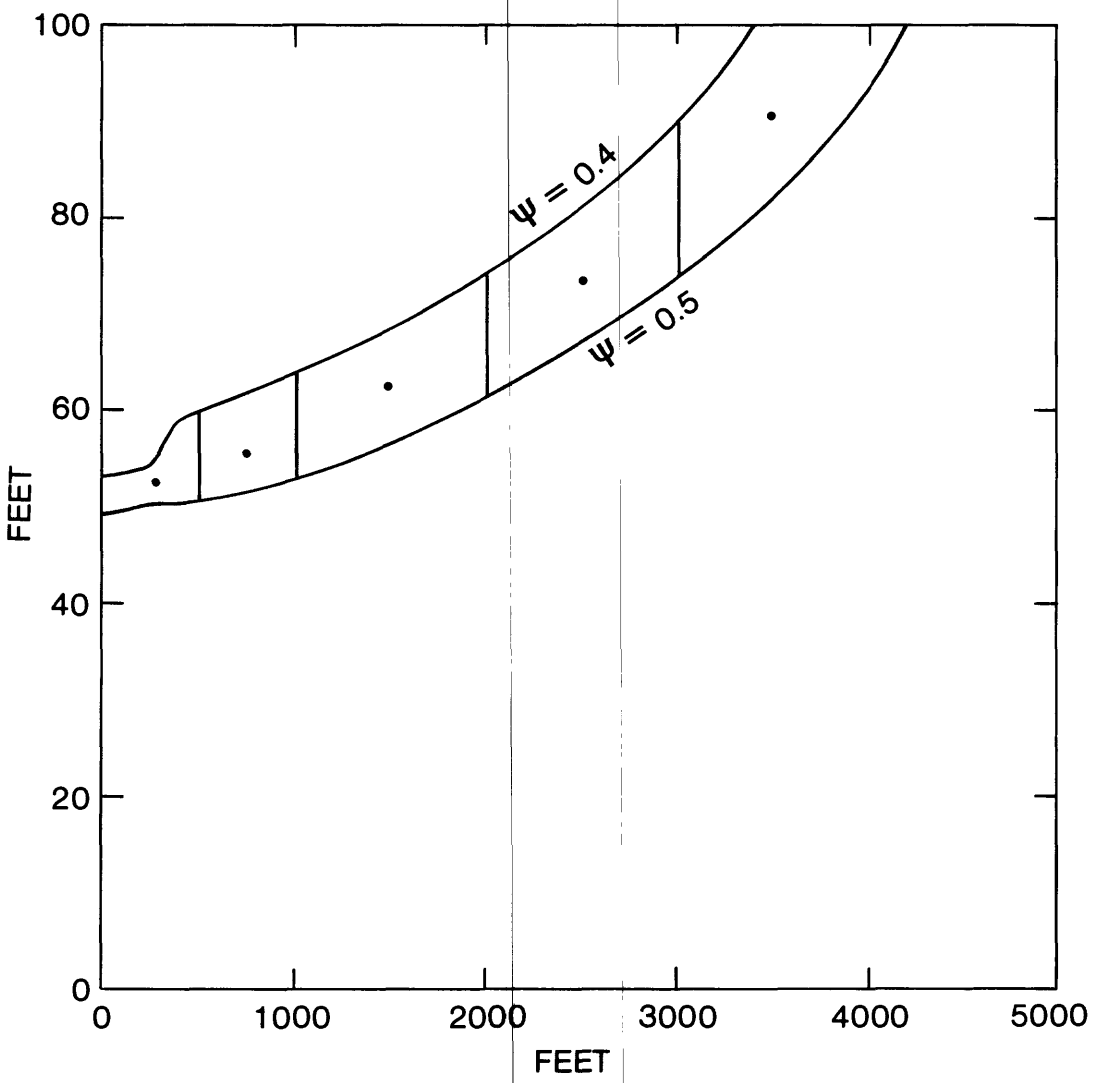

Figure A-9--Graph of 0.4 to 0.5 flow tube used to calculate areas for time of travel

REFERENCES

Aziz, K. and Settari, A. 1979, Petroleum Reservoir Simulation; Applied Science Publishers, Ltd., London, 476 p.

Bennett, Gordon D., 1976, Introduction to ground-water hydraulics--a programmed text for self-instruction: Techniques of Water-Resources Investigations of the United States Geological Survey, Book 3, Chapter B2, 172 p.

Boulton, N.S., 1954, The drawdown of the water-table under non-steady conditions near a pumped well in an unconfined formation: Inst. Civil Engineers (British) Proceedings, v. 3, p. 564-579.

Boulton, N.S., 1963, Analysis of data from non-equilibrium pumping tests allowing for delayed yield from storage: Inst. Civil Engineers (British) Proceedings, v. 26, p. 469-482.

Hantush, M.S., 1960, Modification of the theory of leaky aquifers: Journal of Geophysical Research, v. 65, no. 11, p. 3713-3725.

Hantush, M.S., 1961, Aquifer tests on partially penetrating wells: American Society of Civil Engineers Proceedings, v. 87, no. HY5, p. 171-195.

Hantush, M.S., and Jacob, C.E., 1955, non-steady radial flow in an infinite leaky aquifer: American Geophysical Union Transactions, v. 36, no. 1, p. p. 95-100.

Jacob, C.E., 1946, Radial flow in a leaky artesian aquifer: American Geophysical Union Transactions, v. 27, no. 2, p. 198-205.

Jacob, C.E., and Lohman, S.W., 1952, Nonsteady flow to a well of constant drawdown in an extensive aquifer: American Geophysical Union Transactions, v. 33, no. 4, p. 559-569.

Kirkham, Don, 1959, Exact theory of flow into a partially penetrating well: Journal of Geophysical Research, v. 64, no. 9, p. 1317-1327.

Neuman, S. P., 1972, Theory of flow in unconfined aquifers considering delayed response of the water table: Water Resources Research, v. 8, no. 4., p. 1031-1045.

Reilly, T. E., 1984, A Galerkin finite-element flow model to predict the transient response of a radially symmetric aquifer: U.S. Geological Survey Water-Supply Paper 2198, 33 p.

Theis, C.V., 1935, The relation between the lowering of the piezometric surface and the rate and duration of discharge of a well using ground-water storage: American Geophysical Union Transactions, v. 14, p. 519-524.